

FORMATION OF MASSIVE GALAXIES AT HIGH REDSHIFT: COLD STREAMS, CLUMPY DISKS, AND COMPACT SPHEROIDS

AVISHAI DEKEL, RE'EM SARI AND DANIEL CEVERINO
Racah Institute of Physics, The Hebrew University, Jerusalem 91904 Israel

Draft version November 3, 2018

ABSTRACT

We present a simple theoretical framework for massive galaxies at high redshift, where the main assembly and star formation occurred, and report on the first cosmological simulations that reveal clumpy disks consistent with our analysis. The evolution is governed by the interplay between smooth and clumpy cold streams, disk instability, and bulge formation. Intense, relatively smooth streams maintain an unstable dense gas-rich disk. Instability with high turbulence and giant clumps, each a few percent of the disk mass, is self-regulated by gravitational interactions within the disk. The clumps migrate into a bulge in $\lesssim 10$ dynamical times, or $\lesssim 0.5$ Gyr. The cosmological streams replenish the draining disk and prolong the clumpy phase to several Gigayears in a *steady state*, with comparable masses in disk, bulge and dark matter within the disk radius. The clumps form stars in dense subclumps following the overall accretion rate, $\sim 100 M_{\odot} \text{yr}^{-1}$, and each clump converts into stars in ~ 0.5 Gyr. While the clumps coalesce dissipatively to a compact bulge, the star-forming disk is extended because the incoming streams keep the outer disk dense and susceptible to instability and because of angular momentum transport. Passive spheroid-dominated galaxies form when the streams are more clumpy: the external clumps merge into a massive bulge and stir up disk turbulence that stabilize the disk and suppress in situ clump and star formation. We predict a bimodality in galaxy type by $z \sim 3$, involving giant-clump star-forming disks and spheroid-dominated galaxies of suppressed star formation. After $z \sim 1$, the disks tend to be stabilized by the dominant stellar disks and bulges. Most of the high- z massive disks are likely to end up as today's early-type galaxies.

Subject headings: galaxies: elliptical and lenticular — galaxies: evolution — galaxies: formation — galaxies: mergers — galaxies: kinematics and dynamics — galaxies: spiral — stars: formation

1. INTRODUCTION

The common picture of galaxy formation assumes that disk galaxies form by gas accretion and they transform into spheroidal stellar systems mostly by major mergers (Toomre & Toomre 1972; White & Rees 1978; Fall 1979; Blumenthal et al. 1984; Mo et al. 1998). The disks are assumed to be the sites of quiescent star formation while the mergers are responsible for intense starbursts as well as subsequent quenching of star formation in the spheroidal merger remnant (e.g., Hopkins et al. 2007). While major mergers do occur, recent high-redshift observations and theoretical developments indicate that this is not the major mode of galaxy formation and the star formation in them (see below).

It appears that the most effective star formers in the Universe were galaxies of baryonic mass $\sim 10^{11} M_{\odot}$ in the redshift range $z \simeq 1.5 - 3$. The typical cases are represented by UV-selected galaxies termed BX/BM (Adelberger et al. 2004) and rest-frame optically selected galaxies termed sBzK (Daddi et al. 2004), which we refer to collectively as massive “Star-Forming Galaxies” (SFGs). Their mean comoving space density is $n \simeq 2 \times 10^{-4} \text{Mpc}^{-3}$ (Tacconi et al. 2008), implying within the standard Λ CDM cosmology that they reside in dark-matter halos of masses $M_{\text{v}} \leq 3.5 \times 10^{12} M_{\odot}$. The SFGs show star-

formation rates of order $100 M_{\odot} \text{yr}^{-1}$ (Genzel et al. 2006; Förster Schreiber et al. 2006; Elmegreen et al. 2007; Genzel et al. 2008; Stark et al. 2008), much higher than the few $M_{\odot} \text{yr}^{-1}$ in today's Milky Way, while their baryonic masses and dynamical times are comparable to the Milky Way's. However, as argued below, their observed properties are incompatible with being ongoing mergers (Shapiro et al. 2008) or merger remnants (Bournaud & Elmegreen 2009). The kinematics of many of the SFGs is consistent with a rotating disk, of circular velocity $V \sim 200 \text{km s}^{-1}$ and high velocity dispersion $\sigma \sim 50 \text{km s}^{-1}$. The typical morphology is of a thick, gas-rich disk, extending to a radius $R_d \sim 10 \text{kpc}$. A unique feature of these galaxies, distinguishing them from low-redshift galaxies, is that the disk tends to be broken into several giant clumps, of $\sim 1 \text{kpc}$ in size and up to a few times $10^9 M_{\odot}$ each, in which most of the star formation occurs (van den Bergh et al. 1996; Elmegreen et al. 2004; Elmegreen & Elmegreen 2005; Förster Schreiber et al. 2006; Genzel et al. 2008). This is why they are sometimes referred to as “chain” or “clump cluster” galaxies. There is evidence that these clumps have formed internally in the disk (Bournaud et al. 2008; van Starckenburg et al. 2008; Shapiro et al. 2008). In many cases there is also a significant central bulge, of a somewhat older stellar population than in the disk clumps (Genzel et al. 2008), but somewhat younger than in regular spirals (Elmegreen et al. 2008c).

In contrast, an ongoing merger is not expected to show the kinematics and morphology of a rotating disk. The

Electronic address: dekel@phys.huji.ac.il
Electronic address: sari@phys.huji.ac.il
Electronic address: ceverino@phys.huji.ac.il

enhanced SFR in a merger is expected to occur either in the two progenitor centers or in the compact coalescing core — not in the outer parts of an extended disk. Merger simulations show that a very wet merger with a special choice of orbital parameters may leave behind a non-negligible disk, but in most cases it is embedded in a more massive stellar spheroid remnant (Springel & Hernquist 2005; Robertson et al. 2006; Robertson & Bullock 2008; Governato et al. 2009; Bournaud & Elmegreen 2009). These disks are expected to be smooth and not fragmented into giant clumps (Robertson & Bullock 2008; Bournaud & Elmegreen 2009). Independently, the space number density of SFGs is higher by about a factor of 4 than the expected density of merger-induced starbursts of comparable SFR (Elmegreen et al. 2007; Jogee 2008; Dekel et al. 2009). It should be noted that the most extreme star formers at high redshift are the dusty, bright Sub-Millimeter Galaxies (SMGs) (Chapman et al. 2004; Tacconi et al. 2008; Wall et al. 2008), with SFRs of hundreds of $M_{\odot} \text{ yr}^{-1}$, but these are rarer cases, with space densities that are lower by an order of magnitude. While a significant fraction of the SMGs could indeed be starbursts induced by major mergers, the much more common SFGs pose the interesting question of how could such massive galaxies form most of their stars so rapidly at early times and through a process other than a major merger. A necessary condition is a steady intense gas supply.

In parallel to the existence of SFGs, observations indicate that the other half of the galaxies of $\sim 10^{11} M_{\odot}$ at $z \sim 2$ are actually compact spheroids of radii ~ 1 kpc in which the SFR is suppressed to below $\sim 10 M_{\odot} \text{ yr}^{-1}$ (Kriek et al. 2006; van Dokkum et al. 2008). It seems that a division of galaxy type into a Blue Cloud and a Red Sequence, reminiscent of the robust bimodality known from lower redshifts (a review in Dekel & Birnboim 2006), is already established by $z \sim 2$. A well developed Red Sequence at $z \sim 2$ is not reproduced by current semi-analytic models of galaxy formation, and cannot be explained by the infrequent major mergers. The open questions are how do so many massive spheroids form so early, why are they so compact, and what is the mechanism responsible for the suppression of star formation in these galaxies.

The gravitational fragmentation of gas-rich, thick turbulent disks into big clumps, and the subsequent migration into a central bulge, have been proposed (van den Bergh et al. 1996; Elmegreen & Elmegreen 2005; Genzel et al. 2008; Bournaud et al. 2008) and successfully simulated for idealized disks in isolation (Noguchi 1999; Immeli et al. 2004b,a; Bournaud et al. 2007). According to Toomre (1964), a disk becomes unstable once its surface density is high enough and the circular velocity and velocity dispersion are sufficiently low. The former is responsible for the local self-gravity and the latter tend to balance gravity against local collapse. Being gaseous helps maintaining a disk configuration because the gas cools while a stellar disk tends to acquire and maintain a high velocity dispersion and thicken with time. If the disk is marginally unstable, and if the velocity dispersion to rotation ratio is high, which is equivalent to having a high disk mass compared to the total mass within the disk radius, the typical

clumps are big. Being massive, the timescale for clump migration into the center, by clump-clump gravitational interactions and by dynamical friction, is short. The isolated simulations showed that the clumps coalesce into a central “classical” bulge (Elmegreen et al. 2008a) in several disk dynamical times, on the order of a few hundred Myr, leaving behind a stable low-surface-density disk.

However, we deduce from the appearance of giant clumps in a significant fraction of the massive galaxies at $z \sim 2$ (e.g., Elmegreen et al. 2007; Tacconi et al. 2008) that in each of these galaxies the clumpy disk configuration should last at least for a period comparable to the age of the Universe at that epoch, ~ 3 Gyr, rather than be a single short episode of migration. The key for making it a long-term phenomenon is, again, a continuous, rapid supply of smooth cold gas that would replenish the disk as it is being drained. The incoming gas should keep the disk at the high density that ensures instability and new clump formation in the disk as the older clumps migrate inward. Indeed, such a continuous gas supply is very natural when the galaxy is considered in a cosmological context at high redshift. Theoretical work (Birnboim & Dekel 2003; Dekel & Birnboim 2006), and hydrodynamical cosmological simulations (Kereš et al. 2005; Dekel & Birnboim 2006; Ocvirk et al. 2008; Dekel et al. 2009), have demonstrated that the galaxies in dark-matter halos of $\sim 10^{12} M_{\odot}$ at $z \sim 2$ are typically Stream-Fed Galaxies, which are built by a few cold narrow streams at rates $\sim 100 M_{\odot} \text{ yr}^{-1}$. Dekel et al. (2009) have found that, on average, two thirds of the stream mass are in rather smooth flows involving only clumps smaller than $\sim 10^{10} M_{\odot}$, leading to mini-minor mergers of mass ratio below 1:10 relative to the existing galaxy. This has been shown to explain the abundance of high-redshift SFGs forming stars at high rates, three-quarters of which not through mergers. We show below that the rather smooth streams allow the continuous replenishment of a disk with high surface density without over-producing a velocity dispersion that could have stabilized the disk or completely destroyed it.

On the other hand, we show that the clumpy component of the incoming streams does stir up the disk and can create a high velocity dispersion. Combined with growing a massive bulge, this may stabilize the disk against the formation of in situ giant clumps. If the high SFR is in the disk clumps, the elimination of these clumps is a quenching mechanism that suppresses the star formation preferentially in galaxies that are fed by clumpy streams and have a high bulge-to-disk ratio.

We thus propose a scenario where the formation of galaxies is driven by cold streams, violent disk instability and the growth of a spheroid. The cosmological cold streams play a major role in this process. When their smooth component dominates, they build up the disks and make them fragment into giant clumps. These in situ clumps give rise to rapid star formation as well as to the formation of compact bulges. In the cases of clump-rich incoming streams, the external clumps help growing a massive spheroid through mergers and thus conspire with this spheroid to stabilize the disk and quench star formation. We argue that these are the two main modes of galaxy formation, dominating the buildup of massive

galaxies at high redshift, where most of the mass has assembled into galaxies and most of the stars have formed.

In this paper we present the theoretical framework for this scenario, via simple analytic estimates of characteristic timescales. In §2 we formulate the basic quantities relevant for giant-clump disk instability in terms of the key parameter δ , the ratio of disk to total mass within the disk radius. In §3 we address the self-regulation of the disk instability by the in situ clumps themselves. In §4 we estimate the timescales for clump migration and disk evacuation. In §5 we discuss the cosmological gas input rate through streams, smooth and clumpy. In §6 we work out the evolution toward a steady state with in situ giant clumps when fed by rather smooth streams. In §7 we address the effect of clump-rich streams in growing a massive spheroid and joining forces with it toward stabilizing the disk and suppressing the SFR. In §8 we refer to the SFR within the disk clumps. In §9 we address the survivability of the in situ clumps, against rapid collapse and against disruption by stellar feedback. In §10 we explain the spatial extent of the clumpy disks and the compactness of the spheroids. In §11 we address the instability of a combined disk if gas and stars and the difference between the disks at high redshift and at low redshift. In §12 we display preliminary maps from the first cosmological simulations that reveal disks in a steady-state giant-clump phase. These high-resolution simulations are analyzed in a companion paper (Ceverino et al. 2009). In §13 we summarize our analysis and discuss its implications.

2. DISK INSTABILITY: GIANT CLUMPS

2.1. Instability Criterion

According to the standard Toomre instability analysis (Toomre 1964; Binney & Tremaine 2008, Chapter 6), a thin rotating gaseous disk becomes unstable to axisymmetric modes once the local gravity overcomes both differential rotation and pressure due to turbulence or thermal motions. This is expressed in terms of the stability parameter Q being smaller than a critical value of order unity,

$$Q = \frac{\sigma_r \kappa}{\pi G \Sigma} < Q_c. \quad (1)$$

Here σ_r is the radial velocity dispersion in the disk (or the gas sound speed if it is larger), Σ is the surface density of the disk, and κ is the epicyclic frequency. The latter is related to Ω , the angular circular velocity at radius r , by $\kappa^2 = r d\Omega^2/dr + 4\Omega^2$. The value of κ ranges from Ω for Keplerian orbits, through $\sqrt{2}\Omega$ for a flat rotation curve, $\sqrt{3}\Omega$ in a uniform disk, to 2Ω for solid-body rotation. We adopt hereafter $\kappa = \sqrt{3}\Omega$, appropriate for high-redshift disks. Note that $\Omega(r)$ is determined by the total gravitational force at r , which can be partly exerted by the disk itself and partly by a more spheroidal mass component. A value of Q below unity guarantees that there are scales of perturbations that are both Jeans unstable and rotation unstable, namely, they are large enough not to be stabilized by pressure ($\lambda > \lambda_J = \sigma_r^2/G\Sigma$), and small enough not to be stabilized by the centrifugal force acting in the frame of the local perturbation due to the disk rotation ($\lambda < \lambda_{\text{rot}} = 4\pi^2 G\Sigma/\kappa^2$ for a cold disk).

For a *thick disk*, the analysis of radial modes is qualitatively similar, as long as the perturbation length scale

is smaller than the radius of the disk and larger than its thickness. It yields a slightly smaller value of the critical value, $Q_c \simeq 0.68$, for an isothermal thick disk (Goldreich & Lynden-Bell 1965a). The pressure in the high-redshift thick disks, where $\sigma_z \sim 50 \text{ km s}^{-1}$, is clearly dominated by macroscopic motions, which we crudely refer to as “turbulence”.

For a *stellar disk*, the instability criterion is similar to a gaseous disk, except that the factor π in the definition of Q is replaced by 3.36 — a negligible difference compared to the other uncertainties in the analysis. Thus, as long as the velocity dispersions of gas and stars are comparable, the instability analysis is valid for the combined system of gas and stars as a whole. We adopt this approximation for our simplified analysis of the high-redshift, gas-dominated disks. Observational evidence for this comes so far only from the thickness of the old stellar disk in “chain” galaxies as indicated by IR measurements, which is comparable to the thickness in the UV, associated with stars in formation and therefore gas (Elmegreen et al. 2009). In §11, we address deviations from this simple case, where we discuss star-dominated disks at lower redshifts.

2.2. Clumps and Transient Features

The characteristic wavelength of the unstable mode is (e.g., Binney & Tremaine 2008, Fig. 6.13)

$$\lambda_c \simeq \frac{2\pi^2 G \Sigma}{\kappa^2}. \quad (2)$$

This is $\simeq 0.5\lambda_{\text{rot}}$ and $\simeq 2\lambda_J$ for $Q \simeq 1$. The ring-like density perturbation is expected to break into lumps, and we take the pre-collapse radius of a typical lump to be $R_c \simeq \lambda_c/4$.

If the timescale for decay of pressure support in the growing perturbations is comparable to or shorter than the disk crossing time Ω^{-1} , the perturbations become gravitationally bound virialized clumps of radii $\lesssim R_c$. If the pressure decay time is longer, the perturbations are stretched by shear on a dynamical timescale and become elongated transient features on a length scale comparable to the disk scale (Goldreich & Lynden-Bell 1965b). For example, Gammie (2001) simulated the case of a thin Keplerian gaseous disk and found that a cooling time as short as $t_{\text{cool}} < 3\Omega^{-1}$ permits the fragmentation into bound clumps. He demonstrated that for $t_{\text{cool}} \gtrsim 3\Omega^{-1}$, the system reaches a gravo-turbulent steady state dominated by transient features in which the cooling is balanced by the dissipation of turbulence, by shocks or via a turbulent cascade to the viscous scale. In our case of a gas-dominated high- σ galactic disk, the gas radiative cooling time is much shorter than the dynamical time¹. We thus expect a $Q < Q_c$ unstable disk to fragment into bound clumps encompassing a certain fraction α of the disk mass. Another fraction of the disk mass is expected to be in transient arm-like density perturbations, partly

¹ The radiative cooling time is $t_{\text{cool}} \simeq 2.6 \times 10^3 n^{-1} T_4 \Lambda_{-22}^{-1} \text{ yr}$, where n is the gas density in atoms per cm^3 , here $n \sim 10$, T_4 is the temperature in 10^4 K , and $\Lambda_{-22}(T)$ is the cooling rate in units of $10^{-22} \text{ K cm}^3 \text{ s}^{-1}$. At $T_4 \gtrsim 1.8$, $\Lambda_{22} \sim 1$, and at lower temperatures it drops sharply: at $T_4 = 1$, $\Lambda_{22} \sim 0.04$, and below it is roughly $\Lambda \propto T^2$. Thus, for any $T > 100 \text{ K}$, the cooling time is much shorter than the dynamical time $\Omega^{-1} \sim 50 \text{ Myr}$.

due to non-axisymmetric modes that could be unstable even for $Q > 1$. If the turbulence dissipation somehow becomes slower than the dynamical time, e.g., because of fragmentation and star formation, the balance shifts from bound clumps to transient arms. In particular, the old stellar component, in which σ does not decay, is expected to be part of the transient features.

Indeed, our simulations (§12) confirm the visual impression from the observed “chain” and “clump-cluster” galaxies that many of the disk clumps have well-defined round boundaries and are gravitationally bound physical entities. The simulations also show that the clumps are embedded in a perturbed disk with elongated transient features, and that a significant fraction of the clump mass is being exchanged with the surrounding arms and disk due to tidal effects. The notion that the clumps are long lived while the arms are transients is supported by the finding that the high-redshift star-forming regions in spiral arms are younger than the stellar populations in the clumps of clump-cluster and chain galaxies (Elmegreen et al. 2009).

2.3. Disk Fraction

We adopt as our basic parameter the fraction of mass in the disk component within the characteristic radius of the disk R_d ,

$$\delta \equiv \frac{M_d}{M_{\text{tot}}}, \quad (3)$$

where the total mass M_{tot} within R_d includes the contributions of the disk and the spheroid of dark matter and stars. The maximum possible value of δ is β , the fraction of baryons including disk and bulge within the disk radius,

$$\delta \leq \beta \equiv \frac{M_{\text{bar}}}{M_{\text{tot}}}. \quad (4)$$

The ratio of disk to total baryonic mass is then $M_d/M_{\text{bar}} = \beta^{-1}\delta$, so that a bulge-less disk is $\delta = \beta$, and a disk-less bulge is $\delta = 0$.

Expressing the circular velocity at R_d as

$$(\Omega R_d)^2 = V^2 \simeq \frac{GM_{\text{tot}}}{R_d}, \quad (5)$$

and using the approximate relation

$$M_d \simeq \pi R_d^2 \Sigma, \quad (6)$$

we obtain a simple expression for Q :

$$Q_c \gtrsim Q \simeq \sqrt{3}\delta^{-1} \frac{\sigma_r}{V}, \quad (7)$$

where we have assumed an isotropic three-dimensional velocity dispersion $\sigma = \sqrt{3}\sigma_r$. The initial clump radius becomes

$$R_c \simeq \frac{\pi}{6} \delta R_d, \quad (8)$$

so the typical clump mass is

$$M_c \simeq \frac{\pi^2}{36} \delta^2 M_d. \quad (9)$$

It would be worthwhile evaluating the likely range of the disk fraction δ and its maximum value β in the SFGs. We note up-front that the observed clumpy disks, with

$Q \sim 1$, rule out naked disks, $\delta = 1$. This would have required an extremely high dispersion, $\sigma \sim V$, more compatible with a spheroid. It would have also implied that the clumps are more massive than the observed clumps. Indeed, β is guaranteed to be less than unity due to the dark-matter contribution to the mass within the disk radius.

What is the typical value of the baryonic fraction β ? While $\beta \simeq 0.5$ in the Milky Way today, current estimates for SFGs at $z \sim 2$ range from 0.5 to 0.8 (Bournaud et al. 2008; Forster Schreiber et al. 2009). One way to crudely estimate β from a theoretical perspective is by relating the disk radius to the halo virial radius R_v via

$$R_d \simeq \lambda R_v, \quad (10)$$

where λ is roughly the halo spin parameter (Fall & Efstathiou 1980; Mo et al. 1998). The average value of λ from cosmological N -body simulations and tidal-torque theory is $\simeq 0.04$ and rather independent of mass and time (e.g., Bullock et al. 2001a). On the other hand, the observed typical radii of $R_d \sim 10$ kpc for the high-redshift clumpy disks and the indicated virial radii of $R_v \simeq 100$ kpc for the halos of these galaxies imply an effective value of $\lambda \simeq 0.1$ for these galaxies (Bouché et al. 2007; Genzel et al. 2008) (see a discussion of this excessive disk sizes in §10). Assuming further, very crudely, that the halo is an isothermal sphere of virial mass M_v hosting a baryonic mass M_{bar} of gas and stars, we can approximate $M_{\text{tot}} \simeq \lambda M_v + M_{\text{bar}}$, and obtain

$$\beta \simeq \frac{f_b}{f_b + \lambda}, \quad (11)$$

where $f_b \equiv M_{\text{bar}}/M_v$ is the baryonic fraction within the virial radius. The value of f_b could be lower than the universal value of $\simeq 0.16$ because of mass loss, e.g., due to supernova-driven winds (Dekel & Silk 1986). For $\lambda \sim f_b \sim 0.1$ we obtain $\beta \simeq 0.5$, and with λ and f_b in the ranges 0.04–0.1 and 0.05–0.15, respectively, the value of β ranges from 0.33 to 0.75. Replacing the crude isothermal sphere with a more realistic NFW profile of a low concentration parameter $C \simeq 4$, as appropriate for halos of the relevant masses at $z \sim 2$ (Bullock et al. 2001b), we obtain inside $0.1R_v$ a value of $\beta \simeq 0.63$. The observational indications and this crude theoretical estimate lead us to adopt $\beta = 0.6$ as our fiducial value.

Eq. (7) with $Q \sim 1$ implies that disk fractions in the range $\delta \sim 0.3 - 0.6$ are consistent with the observed range of velocity dispersions $\sigma_r/V \sim 0.17 - 0.35$ (Genzel et al. 2008). For such values of δ in eq. (9), the typical disk clumps are predicted to involve a few percent of the disk mass each, as observed (Elmegreen et al. 2007; Genzel et al. 2008).

If each clump has contracted by a factor of two from its initial radius into virial equilibrium, the internal one-dimensional velocity dispersion within the clump, given by $\sigma_c^2 \simeq (1/3)GM_c/(0.5R_c)$, can be written using eq. (8) and (9) as

$$\frac{\sigma_c}{V} \simeq \frac{\sqrt{\pi}}{3} \delta. \quad (12)$$

Since the radial velocity dispersion of the clumps relative to each other, based on eq. (7), obeys $\sigma_r/V \simeq \delta Q/\sqrt{3}$, we conclude that $\sigma_c \simeq \sigma_r$ when $Q \sim 1$.

3. SELF-REGULATED CLUMPY DISK

For a disk of a given surface density in a given potential well, namely given Σ and Ω , the instability provides a feedback loop that can drive an unstable disk into a self-regulated, marginally unstable state, where $Q \sim Q_c$ and the clumps are as massive as they could be. This means that the velocity dispersion σ_r is kept at the maximum possible value for which Q is still below the critical value for rapid instability. This self-regulation is achieved if the instability and fragmentation process itself is the generator of velocity dispersion, and if it is capable of doing so on a timescale comparable to the timescale of turbulence decay. Then, if σ_r is temporarily low such that Q falls below Q_c , the fragmentation becomes more efficient and it drives Q up toward Q_c . If σ_r overshoots to high values such that $Q > Q_c$, the disk becomes stable, the fragmentation process is suppressed, and σ is allowed to drop such that Q settles to a value just below Q_c .

The turbulence of a gaseous disk dissipates by shocks and by a turbulent cascade to the viscous scale. With a turbulence energy of $E \sim (3/2)M\sigma_r^2$, and for a dissipation rate of $\dot{E} \sim M\sigma_r^3/R_{\text{eddy}}$ where R_{eddy} is the radius of the largest eddy, the dissipation timescale is $t_{\text{dis}} \sim (3/2)R_{\text{eddy}}/\sigma_r$. If $R_{\text{eddy}} \simeq R_c$, and we denote the disk dynamical crossing time by

$$t_d \equiv \Omega^{-1} = \frac{R_d}{V}, \quad (13)$$

we obtain from eq. (8)

$$t_{\text{dis}} \simeq 1.4 Q^{-1} t_d. \quad (14)$$

For Q of order unity, the dissipation timescale is on the order of the disk dynamical time, with no explicit dependence on α or δ . In order to maintain a self-regulated marginally unstable state, the stirring up of turbulence must occur on a comparable timescale.

In an unstable disk with $Q < 1$, the density perturbations grow as $e^{|\omega|t}$, where ω obeys the dispersion relation (e.g., Binney & Tremaine 2008, eq. 6.66)

$$\omega^2 = \kappa^2 - 2\pi G \Sigma |k| + \sigma_r^2 k^2. \quad (15)$$

One can see that the wave number of the fastest growing mode is $k = \pi G \Sigma / \sigma_r^2$, and the growth rate of this mode is given by $\omega^2 = \kappa^2 - (\pi G \Sigma / \sigma_r)^2$. This growth rate, which vanishes for $Q = 1$, becomes comparable to the dynamical time for values of Q slightly below unity, e.g., $|\omega| = \Omega$ for $Q = 1/\sqrt{2}$ (assuming $\kappa = \sqrt{3}\Omega$). The system should maintain a value of Q in this ballpark slightly below unity in order for the fragmentation to react in time to variations in the turbulence level.

What is the mechanism that stirs up the disk and maintains the required velocity dispersion? Some turbulence is generated by feedback from stars and supernovae (§9). Turbulence is also generated by dense gas clumps that flow in as part of the cold streams, but this process is not self-regulated and may stabilize the disk (see §7). However, the highly perturbed fragmented disk is capable of self-regulating itself by the gravitational interactions within it, without the help of external energy sources, and thus maintain the disk in the marginally unstable state. One particular mechanism of this sort for generating velocity dispersion in the

disk is the gravitational encounters between the bound disk clumps (see Wada et al. 2002; Agertz et al. 2008; Tasker & Tan 2009). We demonstrate below that these clump encounters by themselves may be sufficient for self-regulating the disk instability.

The timescale for the clump encounters to generate the velocity dispersion required for a given value of Q can be estimated as follows. First, given that the disk thickness is roughly $(\sigma_z/V)R_d$, with a vertical velocity dispersion $\sigma_z \simeq \sigma/\sqrt{3}$, the spatial number density of clumps is

$$n_c \simeq \frac{\alpha M_d/M_c}{\pi R_d^3 \sigma_z/V}, \quad (16)$$

where α is the fraction of the disk mass that is in clumps at a given time. Second, the cross section for encounters that involve an energy change of order σ^2 can be estimated by²

$$\tilde{\sigma} \simeq \pi(GM_c/\sigma^2)^2. \quad (17)$$

Then, the characteristic time for the encounters to generate a specific energy change $\sim \sigma^2$ is estimated by $t_{\text{enc}} \simeq (n_c \tilde{\sigma} \sigma)^{-1}$. Using eqs. (5), (7) and (9), we obtain

$$t_{\text{enc}} \simeq 2.1 \alpha^{-1} Q^4 t_d. \quad (18)$$

Recall that this expression is valid for Q of order unity, but note the strong dependence of t_{enc} on slight deviations of Q from unity, with no explicit dependence on δ . The kinetic energy of the gaseous clumps could be dissipated in head-on collisions, but the cross section for such collisions is smaller by a geometrical factor of order a few than the cross section for effective gravitational encounters. We therefore expect the net effect of clump encounters to be of stirring up the dispersion on the timescale estimated in eq. (18).

Self-regulation could be obtained by clump encounters alone if $t_{\text{enc}} \sim t_{\text{dis}}$, i.e., $\alpha^{-1} Q^5 \sim 0.67$ when comparing eqs. (18) and (14). This is valid, for example, when $Q \sim 0.67$ and $\alpha \sim 0.2$. Recall that Q is expected to be slightly below unity in the self-regulated unstable state both because $Q_c \simeq 0.68$ is the critical value for instability of a thick disk and because such a value of Q allows perturbation growth on a dynamical timescale. Independently, preliminary observations and simulations (Elmegreen & Elmegreen 2005; Elmegreen et al. 2007; Ceverino et al. 2009) indicate that the value of α can range from 10% to 40%. A value of α in this ballpark could indeed be expected if the unstable wavelength along the tangential direction is comparable to the radial wavelength λ_c , and if clumps form at the regions of positive interference of the tangential and radial waves. We thus adopt $Q \simeq 0.67$ and $\alpha \simeq 0.2$ as our fiducial case.

If the dissipation timescale somehow becomes significantly longer than the disk dynamical time, the balance between dispersion generation by clump encounters and turbulence decay is obtained over a timescale longer than t_d . Such a slowdown of the dissipation rate may result

² If the clump internal velocity dispersion σ_{int} was smaller than the clump-clump velocity dispersion σ , the cross section for the most effective individual encounter was actually πR_c^2 , which is larger by a factor $(\sigma/\sigma_{\text{int}})^4$, but the energy change in each encounter was smaller by a similar factor. Therefore, eq. (17) is indeed the effective cross section for a total change of $\sim \sigma^2$ in a series of such encounters.

from the development of inhomogeneities and fragmentation of the disk gas, through the increase in size of the largest eddies and the possible decrease in cross section for eddy collisions. It may also happen when the stellar component of the disk becomes substantial, as t_{dis} is inversely proportional to the gas fraction in the disk. In this case of slower dissipation the self-regulation in the marginally unstable state can be achieved by clump encounters with a slightly larger value of Q and/or a lower value of α .

The gaseous component between the clumps is expected to participate in the instability and fragmentation process and thus to share the stirred-up clump velocity dispersion. This is especially true for the large-scale transient features, which participate in the stirring up process as they are sheared and stirred up themselves. The inclusion of such additional stirring-up effects may be analogous to increasing α in the analysis of clump encounters above.

4. CLUMP MIGRATION AND DISK EVACUATION

The same clump interactions that generate velocity dispersion, and the dynamical friction exerted by the rest of the disk on the giant clumps, also affect the systematic rotation velocity of the clumps and make them migrate into the center. Both the smooth and clumpy components of the disk are participating in this process, so α should be replaced by unity for the purpose of estimating the migration time. Since the disk just outside a given clump has systematically lower angular velocity, it drains angular momentum from the clump. Over a timescale of αt_{enc} , it would systematically reduce the angular velocity of the clump by σ and therefore cause it to migrate on a timescale $\alpha(V/\sigma)t_{\text{enc}}$. However, the inner disk pushes the clump systematically outward on a similar timescale. The net effect acts on a timescale longer by (V/σ) than that of each side of the disk alone (Goldreich & Tremaine 1980; Ward 1997) The migration time is thus

$$t_{\text{mig}} \simeq \alpha \left(\frac{V}{\sigma} \right)^2 t_{\text{enc}} \simeq 2.1 Q^2 \delta^{-2} t_d. \quad (19)$$

Note that the migration is rapid when Q is low and when δ is high, namely when the disk is massive and unstable, but the migration timescale does not depend explicitly on α .

Given that only a fraction α of the disk is in the giant clumps, the evacuation rate by clump migration of a mass comparable to the entire disk mass is

$$\dot{M}_{\text{evac}} \simeq \frac{\alpha M_d}{t_{\text{mig}}}, \quad (20)$$

and the timescale for the evacuation of the entire disk mass is

$$t_{\text{evac}} \simeq \alpha^{-1} t_{\text{mig}} \simeq 10.5 \alpha_{.2}^{-1} Q^2 \delta^{-2} t_d, \quad (21)$$

where $\alpha_{.2} \equiv \alpha/0.2$. With $Q = 0.67$ and a dominant disk of $\delta = 0.35$, say, we have $t_{\text{mig}} \simeq 7.6 t_d$. Then with $\alpha = 0.2$, the evacuation time is $t_{\text{evac}} \simeq 38 t_d$. With $t_d \simeq 50$ Myr, we obtain $t_{\text{mig}} \simeq 380$ Myr and $t_{\text{evac}} \simeq 1.9$ Gyr. These estimates are consistent with the findings in simulations of isolated disks (Bournaud et al. 2007). When δ is slightly smaller, the timescales are

somewhat longer, consistent with observational estimates (Elmegreen & Elmegreen 2005).

The angular-momentum transfer and mass flow in the perturbed disk involve several other processes beyond the clump-clump interactions and dynamical friction. For example, the clumps induce transfer of disk angular momentum outward, causing much of the disk to accrete inward at a rate that is comparable to the mass inflow rate directly associated with the clump migration itself (Sari & Goldreich 2004). This accretion rate exceeds the migration rate by $d/h \gtrsim 1$, where d is the distance along the disk at which density waves shock and dissipate and h is the vertical scale height of the disk.

The sheared transient features, which are also present in the unstable disk, exert torques which also cause angular-momentum transfer from the inside out. The associated mass inflow rate, based on Shakura & Sunyaev (1973), is

$$\dot{M}_{\text{shear}} \simeq 3^{3/2} G^{-1} \sigma_r^3 Q^{-1} \tilde{\alpha}, \quad (22)$$

where $\tilde{\alpha}$ is the dimensionless angular-momentum flux density. According to Gammie (2001), it is given by

$$\tilde{\alpha} = [(9/4)\tilde{\gamma}(\tilde{\gamma} - 1)\Omega t_{\text{dis}}]^{-1}, \quad (23)$$

where $\tilde{\gamma}$ is the adiabatic index in the equation of state. For $\tilde{\gamma} = 5/3$, appropriate for a turbulent medium, and with $\Omega t_{\text{dis}} \simeq 3$ providing the maximum effect, we have $\tilde{\alpha} \simeq 0.13$. The timescale for evacuating the entire disk by the inflow associated with the transient features becomes

$$t_{\text{shear}} \simeq 7.5 Q^{-2} \delta^{-2} t_d. \quad (24)$$

With $Q \simeq 0.67$, this is three times longer than the disk evacuation time by clump migration, eq. (21), but with Q closer to unity the two evacuation times become comparable.

We thus conclude that by considering only the clump migration, ignoring the other processes causing mass inflow, we obtain an order-of-magnitude estimate for the disk evacuation rate that can serve as a lower limit to the actual evacuation rate.

5. COSMOLOGICAL INPUT RATE BY STREAMS

The key to understanding the high abundance of massive disks with giant clumps at high redshift, as well as the high SFR in them, is the continuous vigorous input of gas into these disks via cold streams. The average relative accretion rate into halos of mass M in the standard Λ CDM cosmology is given to a good approximation by

$$\frac{\dot{M}}{M} \simeq 0.47 (1+z)_3^{2.25} M_{12}^{0.15} \text{ Gyr}^{-1}, \quad (25)$$

where $(1+z)_3 \equiv (1+z)/3$ and $M_{12} \equiv M_v/10^{12} M_\odot$. This has been derived by Neistein et al. (2006) as a useful fit to an analytic prediction based on the EPS approximation and it has been shown to fit well the halo growth rate measured in the Millennium cosmological N-body simulation (Neistein & Dekel 2008; Genel et al. 2008). Dekel et al. (2009) have shown using cosmological hydrodynamical simulations that at high redshift the same expression approximates the average relative baryonic input rate by cold streams into the disks of galaxies of a given baryonic mass, $\dot{M}_{\text{bar}}/M_{\text{bar}}$. The actual accretion rates into individual galaxies range from three times

lower than the average to twice the average. A fraction γ of the stream mass is in clumps of mass larger than $0.1M_{\text{bar}}$, with an average of $\gamma \simeq 0.33$ and an effective range from $\gamma \ll 1$ to γ as high as $\simeq 0.6$ (we denote $\gamma_{.33} \equiv \gamma/0.33$). The rest is in a smoother form consisting of mini-minor gas-dominated clumps and smooth gas in unknown proportions because of limited resolution in the simulations.

We wish to relate this accretion rate to the disk dynamical crossing time, which can be written as $t_{\text{d}} = 48 t_{48} \text{Myr}$. A dynamical time of 48 Myr is obtained for a disk radius $R_{\text{d}} = 10 \text{kpc}$ and a rotation velocity $V = 200 \text{km s}^{-1}$, which are the typical values of $\sim 10^{11} M_{\odot}$ SFGs at $z \sim 2$. Then, eq. (25) defines the accretion time,

$$t_{\text{acc}} \equiv \frac{M_{\text{bar}}}{\dot{M}_{\text{bar}}} \simeq 44 \tau^{-1}(z, M) t_{\text{d}}, \quad (26)$$

where the explicit redshift dependence and the weak mass dependence are in the factor

$$\tau(z, M) = t_{48} (1+z)^{2.25} M_{12}^{0.15}. \quad (27)$$

Note that $\tau \sim 1$ for the typical SFGs at $z \sim 2$. As long as the relevant SFG disks are observed to have similar radii and velocities at different redshifts, namely similar dynamical times, eq. (27) is useful for describing the redshift dependence of t_{acc} .

Alternatively, it could be useful to use $R_{\text{d}} = \lambda R_{\text{v}}$, as in eq. (10), if λ is rather constant in some redshift range, as deduced from cosmological simulations and tidal-torque theory (e.g., Bullock et al. 2001a). If the characteristic disk rotation velocity is comparable to the virial velocity, we have $t_{\text{d}} \simeq \lambda t_{\text{v}}$, where $t_{\text{v}} \equiv R_{\text{v}}/V_{\text{v}}$ is the halo virial crossing time. The cosmological relation between halo virial radius and virial velocity³ implies that τ of eq. (27) can be alternatively expressed as

$$\tau(z, M) = \lambda_{.1} (1+z)^{0.75} M_{12}^{0.15}, \quad (28)$$

where $\lambda_{.1} \equiv \lambda/0.1$. Note that if λ is constant in time, as opposed to t_{d} being constant, the redshift dependence of t_{acc} is weaker. The two expressions for τ , eqs. (27) and (28), coincide at $z \simeq 2$ for $t_{48} = \lambda_{.1} = 1$. Based on the observed SFGs, it seems that the disk dynamical time is roughly constant at lower redshifts $z \leq 2$. On the other hand, a constant λ may be more sensible from a theoretical point of view at $z \geq 2$ (see a discussion of disk sizes in §10 below).

At $z = 2$, when the cosmological time is $t_{\text{H}} \simeq 3.25 \text{Gyr}$, the virial crossing time is $t_{\text{v}} \simeq 0.48 \text{Gyr}$ and $t_{\text{acc}} \simeq 2.1 \text{Gyr}$ compared to the disk dynamical time of $t_{\text{d}} \simeq 48 \text{Myr}$.

³ For the standard ΛCDM cosmology ($\Omega_{\text{m}} = 0.28$, $\Omega_{\Lambda} = 0.72$, $h = 0.7$), in its Einstein-deSitter regime, $z > 1$, the standard virial radius and velocity are related to the virial mass as $R_{\text{v}} \simeq 308 \text{kpc} (1+z)^{-1} M_{12}^{1/3}$ and $V_{\text{v}} \simeq 118 \text{km s}^{-1} (1+z)^{1/2} M_{12}^{1/3}$. Thus $V_{200} \simeq R_{100} (1+z)^{3/2}$, where the quantities are in units of 200km s^{-1} and 100kpc , respectively. The virial crossing time is roughly a constant fraction of the Hubble time, $t_{\text{v}} \simeq 0.15 t_{\text{H}}$. In this regime the inverse of the expansion factor can be approximated by $(1+z) \simeq 6.6 t_{\text{H}}^{-2/3}$, where the Hubble time t_{H} is in Gigayears.

6. COSMOLOGICAL STEADY STATE

6.1. Evolution Equation

The high number density of massive SFGs that appear to be rotating disks broken into giant clumps indicates that they constitute a large fraction of the galaxies in halos of $\sim 10^{12} M_{\odot}$ at $z \sim 2$. This implies that the presence of giant clumps is not a short episode in the galaxy lifetime that disappears in one migration time, on the order of 400 Myr, but rather a long-term phenomenon that lasts for a Hubble time, on the order of 3 Gyr or more. The key for a long-lived disk with giant clumps is, again, the continuous, intensive gas supply into the disk by cold and rather smooth streams, valid at high redshift (Dekel et al. 2009).

We wish to work out how δ evolves in time, as the disk is being built and drained and as the bulge grows. The time derivative $\dot{\delta}$ can be derived from

$$\delta = \beta \frac{M_{\text{d}}}{M_{\text{bar}}}. \quad (29)$$

The baryon growth rate \dot{M}_{bar} is the total baryonic accretion rate from eq. (26), and the rate of change of disk mass, \dot{M}_{d} , is the difference between input to the disk and output from it,

$$\dot{M}_{\text{d}} \simeq (1 - \gamma) \dot{M}_{\text{bar}} - \dot{M}_{\text{evac}}(\delta), \quad (30)$$

with $\dot{M}_{\text{evac}}(\delta)$ from eqs. (19) and (20). For completeness, the associated growth rate of the bulge is

$$\dot{M}_{\text{sph}} \simeq \gamma \dot{M}_{\text{bar}} + \dot{M}_{\text{evac}}(\delta). \quad (31)$$

The factor γ allows for the possibility that only the smooth fraction $(1 - \gamma)$ of the incoming streams adds to the disk mass, while the more massive clumps along the streams merge into the spheroid independent of the disk instability; that is, a standard merger. One assumes here that, on their way to join the bulge, those massive external clumps do not spend a significant amount of time as proper disk members (with a circular velocity V and a dispersion σ) compared to the rest of the disk material. They therefore do not increase the disk surface density and thus do not speed up the migration and evacuation of the in situ clumps. This assumption is justified because the massive external clumps are several times more massive than the internal disk clumps, and their effective masses are even larger because they are likely to carry with them dark matter, so their inward migration time by dynamical friction is much shorter than the disk evacuation time. From the simulation analyzed by Dekel et al. (2009), we learn that the average value of $\gamma \simeq 0.33$ refers to external clumps more massive than $0.1M_{\text{bar}}$. This could perhaps serve as a crude estimate for the dividing line between “massive” stream clumps that lead to major or minor mergers without joining the disk, and the smoother component involving “mini-minor” clumps that do join the disk and spend a non-negligible time there. We estimate further, based on the simulation, that about a third of the galaxies are fed by smooth streams of $\gamma \ll 1$, and another third have an excess of massive incoming clumps, $\gamma \gtrsim 0.5$.

As a simple example, we work out the case $\beta = \text{const.}$, following the notion that the virial baryonic fraction f_{b} and the effective spin parameter λ that enter eq. (11)

are constant in time. The gas input rate is assumed to follow the cosmological mean for that mass and redshift. We also assume for simplicity that M_v remains in the broad range $10^{11} - 10^{12.5} M_\odot$, taking advantage of the very weak mass dependence of the accretion time and the dynamical time. Using the definitions eqs. (21) and (26) in eq. (30), we obtain for the rate of change of δ

$$\dot{\delta} \simeq \beta(1 - \gamma - \beta^{-1}\delta)t_{\text{acc}}^{-1} - \delta t_{\text{evac}}^{-1}(\delta), \quad (32)$$

in which the δ -dependence is explicitly specified. We intend to solve this differential equation for $\delta(t)$.

6.2. Steady State Attractor

We first note that for a given accretion rate, there should be a steady-state configuration where $\dot{\delta} = 0$; that is, δ remains fixed at a critical value, δ_{ss} . This configuration serves as an ‘‘attractor’’: if $\delta > \delta_{\text{ss}}$, the efficient disk evacuation and spheroid growth make δ decline toward δ_{ss} , and if $\delta < \delta_{\text{ss}}$, the efficient streaming into the disk forces δ up back to δ_{ss} . In order to estimate the value of δ_{ss} , we set $\dot{\delta}$ to zero in eq. (32), namely

$$\frac{t_{\text{acc}}}{t_{\text{evac}}(\delta_{\text{ss}})} \simeq \beta(1 - \gamma)\delta_{\text{ss}}^{-1} - 1. \quad (33)$$

The relevant time ratio, from eqs. (21) and (26), is

$$\frac{t_{\text{acc}}}{t_{\text{evac}}} \simeq 4.18 \alpha_{.2} Q^{-2} \tau^{-1} \delta^2, \quad (34)$$

so, the equation is a depressed cubic polynomial equation for δ_{ss} ,

$$\delta_{\text{ss}}^3 + b\delta_{\text{ss}} - c = 0, \quad (35)$$

$$b \equiv 0.24 \alpha_{.2}^{-1} Q^2 \tau, \quad c \equiv b\beta(1 - \gamma). \quad (36)$$

The solution (e.g., by Cardano’s method) is

$$\delta_{\text{ss}} = u - \frac{b}{3u}, \quad (37)$$

$$u = \left(\frac{c}{2}\right)^{1/3} \left[1 + \left(1 + \frac{4b^3}{27c^2}\right)^{1/2} \right]^{1/3}. \quad (38)$$

With the fiducial values $Q = 0.67$, $\alpha = 0.2$ and $\beta = 0.6$, and with γ in the range $0 - 0.33$, we obtain at $z = 2$,

$$\delta_{\text{ss}} \simeq 0.32 - 0.25. \quad (39)$$

Simple solutions of eq. (35) in certain limits are discussed in §A.

The redshift dependence of δ_{ss} is rather weak. For example, with $\gamma = 0$, we obtain $\delta_{\text{ss}} \simeq 0.38$ and 0.25 at $z = 9$ and 1 , respectively (where we have assumed $\lambda \simeq 0.1$ at $z \geq 2$ and $t_d \simeq 48$ Myr at $z \leq 2$). The mass dependence is even weaker. Varying β in the range $0.5 - 0.75$ yields $\delta_{\text{ss}} \simeq 0.28 - 0.35$. Varying α in the range $0.1 - 0.4$ gives $\delta_{\text{ss}} = 0.37 - 0.26$. We see that when varying the parameters within their likely ranges about the fiducial values, the value of δ_{ss} at $z \sim 2$ remains quite stable about 0.3 . Thus, the steady-state configuration is expected to be with a bulge mass comparable to the disk mass, $\delta \simeq \beta/2$, to within a factor of two.

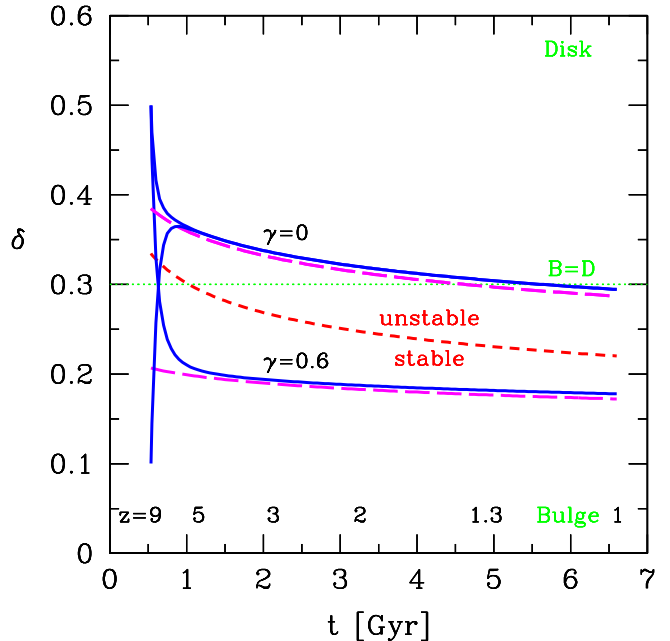


FIG. 1.— Steady state and bimodality. The solid blue curves show the evolution of the disk-to-total mass ratio δ , according to eq. (32), for the fiducial case ($Q = 0.67$, $\alpha = 0.2$, $\beta = 0.6$, $t_d = 0.015 t$ and an average cosmological inflow rate). Shown are two extreme cases in terms of the presence of massive clumps in the incoming streams: very smooth streams ($\gamma = 0$) and very clumpy streams involving mergers ($\gamma = 0.6$). Eq. (32) is solved starting at $z = 9$ with either a dominant disk ($\delta = 0.5$) or a dominant bulge ($\delta = 0.1$). Independent of the initial configuration, as long as the disk is unstable the system converges within less than a Hubble time to a quasi-steady state where δ is slightly above δ_{ss} (long-dashed magenta curves). The critical value for stabilization by incoming stream clumps, δ_{stab} of eq. (43), is shown as a dashed red curve for $\gamma_c = 0.33$ and $v = 1.2$. It implies that streams that are smoother than average ($\gamma < 0.33$) produce a long phase of an unstable giant-clump disk with a comparable bulge that can last till after $z \sim 1$. Streams that are more clumpy than average ($\gamma > 0.33$) stabilize the disk and lead to a bulge-dominated system with a less massive, smoother disk. Therefore, the actual solution for $\gamma = 0.6$ deviates from the lower curve shown.

6.3. Convergence to Steady State

With the average accretion rate evolving on a timescale that is not much longer than the disk evacuation timescale, we need to verify that the system indeed approaches a quasi-steady state, and find out how far it might be from δ_{ss} where $\dot{\delta} = 0$. Figure 1 shows numerical solutions for $\delta(t)$ of eq. (32) with eq. (34), for the fiducial choice of parameters and $t_d = 0.015 t$, eq. (28). The initial conditions are set, as an example, at the reionization epoch, $z_{\text{in}} \simeq 9$ or $t_{\text{in}} \simeq 0.54$ Gyr. We choose the starting configuration to be alternatively disk dominated, $\delta_{\text{in}} = 0.5$, or bulge dominated, $\delta_{\text{in}} \ll 1$. Independent of the initial conditions, the system settles within a Hubble time to a value of δ near δ_{ss} , which is also shown. This can be understood via the approximate solutions to eq. (32) discussed in §A. The actual steady-state value of δ is slightly higher than δ_{ss} because the latter declines with time on a timescale that is somewhat larger than the timescale for changes in δ , driven in this range by t_{evac} .

We conclude that throughout the broad redshift range of interest the system tends to be in a steady state in

which the bulge and disk masses are comparable, to within a factor of two. The disk fraction in this steady state is larger in cases where the fraction of massive clumps in the incoming streams is smaller. Note that the evolution curves shown in Fig. 1 are derived, so far, under the assumption that the disk is always unstable to the formation of giant clumps. We will see next that this assumption may be valid only for streams that are smoother than average, namely a low γ and then a high δ . An excess of incoming stream clumps may stir up the disk to stabilization with a low value of δ .

The observed high-redshift SFGs indeed seem to indicate convergence into a steady state with a bulge of mass comparable to the disk mass, $\delta \sim 0.3$, as predicted here. Genzel et al. (2008, and private communication) have measured for six SFGs the “concentration” C , defined as the ratio of total dynamical masses within the radii of $0.4''$ and $1.2''$, which roughly correspond to $(1/3)R_d$ and R_d , respectively. Allowing for 20% of the mass within the inner radius to come from dark matter and disk (appropriate for an NFW halo profile and a uniform disk profile), the observed value of $0.8C$ could be interpreted as the bulge-to-total mass ratio within the disk radius, $0.8C \simeq \beta - \delta$. When they plot in Fig. 5 the value of C against the time t_* of onset of star formation in that galaxy⁴, they find that C is rising monotonically with t_* for $t_* < 0.5$ Gyr until it settles to a rather constant value near $C \simeq 0.38$ for $t_* \simeq 0.5 - 2$ Gyr. This is consistent with the quick convergence to a steady state as predicted in Fig. 1, and with the steady-state configuration of $\delta \simeq 0.3$ (for $\beta = 0.6$ and $\gamma < 0.33$), which corresponds to a bulge-to-total ratio $0.8C \simeq 0.3$.

7. STABILIZATION BY EXTERNAL STREAM CLUMPS

Beyond the self-regulated stirring up of the disk by the in situ disk clumps themselves (§3), the incoming streams provide an alternative source for generating velocity dispersion in the disk. Unlike the stirring by the internal products of the disk instability, which is naturally self-regulated, the external source could in principle push σ up to a level that stabilizes the disk.

When a smooth stream of gas density ρ_s hits a disk of much higher gas density ρ_d , conservation of momentum implies that the kinetic energy added to the disk is roughly a fraction ρ_s/ρ_d of the total kinetic energy of the stream, while most of the incoming energy turns into heat that is radiated away. This implies that the smooth component of the streams, which is less dense than the disk by more than an order of magnitude, is not effective in stirring up the disk.

However, the streams contain a clumpy component with gas densities comparable to the disk density. In the impact of such an external dense clump with the disk, about half the kinetic energy is expected to turn into turbulence in the disk. The timescale for stirring up the disk to a given value of σ by external gas clumps that stream in with a velocity V_{in} can thus be estimated by

$$t_{stab} \simeq \frac{M_d \sigma^2}{(\gamma_c/2) \dot{M}_{bar} V_{in}^2}. \quad (40)$$

⁴ t_* is the time to form the current stellar mass at a constant SFR that equals the current SFR — a model that fits the data well (Forster Schreiber et al. 2009)

The assumption here is that incoming clumps that constitute a fraction γ_c of the stream mass share most of their kinetic energy and angular momentum with the disk. This γ_c is not necessarily the same as the γ used in §6 to compute the evolution of an unstable system into a steady state. It may include the same massive clumps, under the assumption that they stir up the disk before they end up merging with the bulge, as well as minor clumps (e.g., less massive than $0.1M_{bar}$), which do not merge quickly with the bulge but are dense enough for stirring up the disk. We defer a more accurate estimate of the fraction of dense clumps in the streams to a future work based on simulations with higher resolution. Meanwhile, for the purpose of the current simplified analysis, we adopt $\gamma_c = 0.33$, the average value deduced from the MareNostrum simulation used in Dekel et al. (2009)⁵. We mark $v \equiv V_{in}/V_v$, and read from the same simulation that on average $v^2 \sim 2$.

We see from eqs. (19) and (21) that $\sigma^2/V^2 \simeq t_{enc}/t_{evac}$, so with t_{acc} from eq. (26), eq. (40) becomes

$$t_{stab} \simeq 2 \gamma_c^{-1} v^{-2} \beta^{-1} \frac{t_{acc}}{t_{evac}(\delta)} \delta t_{enc} \quad (41)$$

$$\simeq 88 \gamma_c^{-1} v^{-2} \beta^{-1} \tau^{-1} Q^2 \delta^3 t_d. \quad (42)$$

The first equality tells us that when the external clump accretion rate is sufficiently higher than the disk evacuation rate, the stirring by external stream clumps is more effective than the stirring by internal disk clumps, which operates on a timescale $\sim t_{enc}$. This generation of turbulence by an external source is not self-regulated and could stabilize the disk if it operates on a timescale that allows it to balance the dissipation of turbulence, namely if $t_{stab} \leq t_{dis}$. Using eqs. (14) and (42), this condition translates to stabilization by external stream clumps once

$$\delta < \delta_{stab} \simeq 0.25 (\gamma_c v^2 \beta \tau)^{1/3} Q^{-1}. \quad (43)$$

Naturally, the disk tends to be stabilized by the streams when the streams contain more dense clumps and the accretion rate is high, and especially when δ is low due a significant contribution from the spheroid. The latter is because a low δ requires a low critical σ for $Q \simeq Q_c$, which makes it easier for a given stream to drive σ above the critical value.

Note that the mass dependence of δ_{stab} , entering through τ in eq. (43), is very weak. For a halo mass smaller by an order of magnitude, δ_{stab} is smaller by $\sim 10\%$. The redshift dependence entering through τ is somewhat more pronounced, but it is still rather weak; it depends on whether t_d or λ are assumed to be constant in time, eqs. (27) or (28), namely $\delta_{stab} \propto (1+z)^{0.75}$ or $(1+z)^{0.25}$, respectively.

Figure 1 shows δ_{stab} for the fiducial case $\gamma_c = 0.33$ and $v = 1.2$. We learn that for average clumpiness, $\gamma \simeq \gamma_c \simeq 0.33$, the value of δ_{stab} happens to be in the ballpark of the steady-state value of δ . The value of $\gamma \simeq 0.33$ thus marks the transition between two very different evolution tracks. In the cases of streams smoother

⁵ It may be interesting to note that Khochfar & Silk (2009) estimate from a semi-analytic model that $\simeq 18\%$ of the stream kinetic energy is required for driving a velocity dispersion as observed, consistent with the $\gamma_c/2$ factor predicted by our theoretical argument, with our average value $\gamma_c \simeq 0.33$.

than average, $\gamma < 0.33$, the stirring by external stream clumps is unimportant, as $\delta > \delta_{\text{stab}}$ at all times. This is especially true for the case $\gamma \ll 1$ shown in the figure. In this case, and as long as the accretion rate follows the cosmological average, the disk is in a long-term giant-clump phase near steady state with δ slightly above δ_{ss} . For $\gamma \ll 1$, the value of δ ranges from $\delta \simeq 0.4$ at very high z to $\delta \simeq 0.3$ at $z \sim 1$, namely the bulge contains between a third and a half of the baryonic mass. This is compatible with the bulges detected in typical SFGs at high redshift, as mentioned at the end of §6.

In the cases where the streams are more clumpy than average, $\gamma > 0.33$, the stabilization by external stream clumps becomes important, as $\delta < \delta_{\text{stab}}$ at all times. The disk does not develop a giant-clump phase (and if it somehow did at very high redshift, it was a short episode). In such a case, the bulge grows predominantly by the merging incoming massive clumps. The system does not evolve according to the evolution track shown in Fig. 1 for $\gamma = 0.6$. Instead, it settles to either $\delta \simeq \delta_{\text{stab}}$ or $\delta = \beta(1 - \gamma)$, whichever is smaller. In this case the bulge is a high fraction of the baryonic mass, on the order of γ .

Our analysis thus predicts a robust *bimodality* in the galaxy population already at high redshift, driven by the spread in the degree of clumpiness in the streams feeding the galaxies. A small deviation of γ from the average value $\simeq 0.33$ triggers a qualitative difference in the evolution pattern, even if the overall mass growth rate follows the cosmological mean. This bimodality is consistent with the observed high abundance of clumpy star-forming, extended disks at $z \sim 2$, alongside with the realization that a significant fraction of the massive galaxies are dominated by compact spheroids and show low SFR already at these redshifts (Kriek et al. 2006; van Dokkum et al. 2008). We predict that many of these high-redshift spheroids are surrounded by smooth, stable disks containing about a third of the baryonic mass, which continue to evolve secularly and form stars quiescently (§11). Such secondary disks are indeed apparent in some of the HST NIC2 images of compact passive spheroidal galaxies at $z \sim 2 - 3$ (van Dokkum et al. 2008, Fig. 1). This configuration, of a dominant compact stellar spheroid and a smooth secondary disk, is not very different from the predicted remnants of certain binary wet major mergers (Springel & Hernquist 2005; Robertson & Bullock 2008; Governato et al. 2009), not to be confused with the extended, high-redshift disks of giant clumps forming stars that are not dominated by the central spheroid (Bournaud & Elmegreen 2009).

The evolution described in Fig. 1 assumes continuous gas input at the average cosmological rate and a constant level of clumpiness in the streams. Time variations in the stream properties can shift a galaxy from an unstable to a stable mode and vice versa. An example is illustrated in the simulated evolution of a Milky-Way-type galaxy termed “Via Lactea”?, Fig. 5, where the overall growth rate drops to below-average levels between $z \simeq 2.5$ and 1.8. As a result, the bulge-to-disk ratio grows and δ drops below δ_{stab} , bringing the unstable giant-clump phase to an end. When the accretion resumes at $z \sim 1.8$, it takes the system a Hubble time, about 4 Gyr, to rebuild a disk that may bring it back to the unstable regime with $\delta > \delta_{\text{stab}}$ after $z \simeq 1$. By that time, the disk is already in the

star-dominated regime and may never resume instability (§11).

8. STAR FORMATION

The observed SFGs of $M_{\text{bar}} \sim 10^{11} M_{\odot}$ at $z \sim 2$ show that the giant disk clumps are the sites of intense star formation. This indicates that the formation of clumps is a necessary condition for the main mode of star formation in high-redshift galaxies. While the physics of this mode of star formation is beyond the scope of the current paper, we discuss here certain implications of our analysis of gas streams and disk instability, combined with the observed overall SFR, on the process of star formation in the clumps.

The observed overall SFR of $\sim 100 M_{\odot} \text{yr}^{-1}$ across the disk (Elmegreen et al. 2007; Genzel et al. 2008) is only slightly smaller than the theoretically predicted gas input rate via cold streams into the central galaxies of dark-matter halos that are comparable in abundance to these SFGs (Dekel et al. 2009). This leads to the approximation that the overall SFR in the disk is a significant constant fraction of the gas accretion rate from eq. (26): $\dot{M}_{*d} \simeq s \dot{M}_{\text{bar}}$ with $s \sim 0.5$. The stars formed earlier in the incoming external clumps are not part of the star formation in the in situ disk clumps.

As a simple model for the SFR in the disk clumps, we assume that the clump mass $M_c = M_g + M_*$ remains constant as it turns gas into stars, and that the SFR in the clump is $\dot{M}_{*c} = M_g/t_*$ with a constant t_* . Then $\dot{M}_{*c}(t) = (M_c/t_*) \exp(-t/t_*)$. This means that most of the stars form during a period $\sim t_*$ with a SFR on the order of M_c/t_* . The fact that a significant fraction of the accreted gas is observed to form stars in the clumps while they are still in the disk implies that t_* is not much longer than the clump migration time t_{mig} . On the other hand, the observations indicate that the number of star-forming big clumps, ~ 5 , is comparable to the number of clumps seen in simulations (§12) and consistent with our fiducial values of M_c and α from the instability analysis. If the clumps survive for a migration time (but see §9.2), this implies that t_* is not much smaller than t_{mig} . We conclude that $t_* \sim t_{\text{mig}}$.

This is consistent with the cosmological steady state (§6.2) because the requirement that the SFR be comparable to the accretion rate is equivalent to the approximate condition for steady state, $t_{\text{evac}} \sim t_{\text{acc}}$. Indeed, if we write $t_* = \alpha M_d / \dot{M}_{*d}$, we obtain

$$t_* \simeq \alpha \beta^{-1} s^{-1} \delta t_{\text{acc}} \quad (44)$$

$$\simeq 8.8 \alpha_{.2} \beta^{-1} s^{-1} \tau^{-1} \delta t_d, \quad (45)$$

which is comparable to t_{mig} from eq. (19) for our fiducial unstable disk with $\delta = 0.3$ at $z \sim 2$, where $t_* \simeq 8.8 t_d \simeq 420 \text{ Myr}$.

Based on the above simple model, the gas fraction in the clump when it coalesces with the bulge is $f_g = \exp(-t_{\text{mig}}/t_*) \simeq e^{-1}$. This implies that the disk clumps merge into the central spheroid while they are still relatively gas rich. The process is thus similar to a wet major merger, where the gas shocks, heats up, cools, and condenses to the center, leading to a compact spheroid significantly smaller than the disk size (e.g., Dekel & Cox 2006; Covington et al. 2008). This may ex-

plain the compactness of observed spheroids at $z \sim 2$ (van Dokkum et al. 2008). In the late phases of spheroid growth, when δ is smaller, t_{mig}/t_* is larger, so the mergers of the disk clumps into the spheroid are less dissipative, making the late-formed spheroids less compact.

The SFR efficiency in the disk clumps, based on eq. (45) and with $t_c \simeq 0.5t_d$, is

$$\eta \equiv \frac{\dot{M}_{*c}}{M_c/t_c} = \frac{t_c}{t_*} \quad (46)$$

$$\simeq 0.06 \alpha_2^{-1} \beta s \tau \delta^{-1}. \quad (47)$$

For the fiducial case, with $\delta \simeq 0.3$ at $z \simeq 2$, we obtain $\eta \simeq 0.06$. Similar high efficiencies were estimated for $z \sim 2$ SFGs based on the pressure in the star-forming clumps (Lehnert et al. 2009). However, such values of η are higher than the efficiencies in the most efficient star-forming clouds at low redshift. The common wisdom, based on the empirical Kennicutt-Schmidt law (Kennicutt 1989) and on star-formation theory (Krumholz et al. 2009), is that η is of order 1% in all star-forming environments, independent of the actual density. This indicates that the giant disk clumps may not form stars uniformly over their whole volume. Instead, stars form with a standard efficiency $\sim 1\%$ in subclumps where the density is two orders of magnitude higher so the local dynamical time is an order of magnitude shorter. This is an observable prediction, to be addressed when the star-forming clumps are resolved.

9. CLUMP SURVIVAL AND DISRUPTION

The appearance of giant gas clumps forming stars in the disks of many SFGs indicates that they survive for at least several dynamical times. The same is evident in simulations (see §12). One wishes to understand the mechanisms that prevent the clumps from collapsing into themselves on a free-fall time and help them survive the various processes that work to disrupt them. In particular, once the disk clumps form stars at high rates, they could be affected by stellar feedback, in the form of supernovae-driven winds or radiative feedback from massive stars, which we briefly comment on below. A preliminary discussion of the possible gravitational origin for the turbulence pressure supporting the clumps is provided in §B.

9.1. Supernova Feedback

Could supernova feedback provide the pressure support against free-fall collapse? If so, is there a risk that supernova-driven winds may remove the remaining gas and disrupt the clumps before they complete their migration? Dekel & Silk (1986) evaluated the maximum energy fed into the interstellar gas by supernovae, taking into account the radiative losses, $E_{\text{SN}} \simeq \epsilon \nu \dot{M}_* t_{\text{rad}}$, where \dot{M}_* refers to the SFR in each clump, ϵ is the energy released by a typical supernova ($\sim 10^{51}$ erg), and ν is the number of supernovae per unit mass of forming stars (which for a typical IMF is $\nu \sim 1$ per $50M_\odot$). The characteristic time t_{rad} marks the end of the “adiabatic” phase and the onset of the “radiative” phase of a typical supernova remnant, by which it has radiated away a significant fraction of its energy and became ineffective. They found that it takes a similar time for the expand-

ing supernova shells to reach a significant mutual overlap, which allows an even distribution of the supernova energy (minus the radiative losses) over most of the gas. A necessary condition for the clump to be significantly affected by supernova feedback is that E_{SN} exceeds the binding energy of the clump, $\sim (1/2)M_c \sigma^2$. This occurs if the potential well associated with the clump is shallow enough, with a three-dimensional velocity dispersion

$$\sigma^2 \leq V_{\text{SN}}^2 = 2 \epsilon \nu \eta \frac{t_{\text{rad}}}{t_d}. \quad (48)$$

It turns out that in the relevant temperature range the cooling rate scales approximately as $\Lambda \propto T^{-1}$, which implies that the ratio of timescales is roughly $t_{\text{rad}}/t_d \sim 0.01$ independent of gas density and other clump parameters. Dekel & Silk (1986) then assumed maximum efficiency in a burst of star formation, $\eta \simeq 1$, and obtained a critical velocity of $V_{\text{SN}} \simeq 100 \text{ km s}^{-1}$ as an upper limit for the virial velocity of a system in which one may expect substantial gas heating or removal by supernova feedback.

With the estimated SFR efficiency of $\eta \sim 0.1$ in each clump as a whole, the critical velocity is reduced to $V_{\text{SN}} \sim 30 \text{ km s}^{-1}$. This implies that supernova feedback cannot be effective in the giant clumps during the steady-state instability phase of a $V \sim 200 \text{ km s}^{-1}$ disk, where $\delta \sim 0.3$ and therefore $\sigma \sim 40 - 60 \text{ km s}^{-1}$ by eq. (7). The clumps may become more vulnerable to supernova feedback, $\sigma < 30 \text{ km s}^{-1}$, once $\delta < 0.2$, namely when the bulge becomes twice as massive as the disk (see also simulations by Tasker & Bryan 2008). However, when the clump fragments, the supernova-driven winds may escape harmlessly via low density “chimneys” through a porous interstellar medium (e.g., Ceverino & Klypin 2009), and thus not lead to disruption even in clumps of σ well below 30 km s^{-1} .

9.2. Radiation Pressure

While supernova feedback may be unimportant in the giant clumps, radiative feedback from O stars may be more effective. Murray et al. (2009) estimate that the clumps should be disrupted by radiative pressure once about 20% of their gas has turned into stars, expelling the remaining 80% of the gas back to the disk. If true, we can deduce that the system would maintain a steady state similar to the one described in §6, with the disk evacuation by migration replaced by an “evacuation” into dense star clusters that do not participate in the disk instability any longer. The two steady states are similar because the timescales for clump migration and for star formation in a clump mass are comparable (§8). The expelled gas, combined with the gas streaming in from the outside, would then help keeping the disk gaseous and unstable.

However, if each clump is disrupted this way, its mass becomes smaller by a factor of ~ 5 , so the bulge buildup by migration becomes slower by a factor of $\sim 5^2$. This is because the migration time is inversely proportional to the clump mass, and the mass added to the bulge by each coalescing clump is proportional to the clump mass. This implies that most spheroids have to be made by mergers, in possible conflict with the cosmological merger rate and with most semi-analytic simulations of galaxy formation (also discussed in §13). On the other hand, this scenario predicts the common existence of massive

thick stellar disks, constructed from the slowly migrating star clusters, which may be associated with today's thick disks and S0 galaxies.

The stellar populations in the high-redshift clumps can provide an observational test that could clarify the survivability of the clumps. With $\eta \sim 0.06$, one fifth of the clump mass becomes stars in about three clump dynamical times, namely ~ 75 Myr. If radiative feedback suppresses star formation after that time, the spread of stellar ages in each clump should not exceed $\sim 50 - 100$ Myr. The slow migration implies that the single-age population in the clumps could be as old as ~ 2 Gyr. In contrast, if the gas clumps survive for a migration timescale, the age spread could be ~ 0.5 Gyr, and giant clumps should not show populations older than ~ 1 Gyr. In this case, we predict that the typical giant clumps should be gas rich and forming stars at a high rate while they also contain a stellar population that has been formed in a similar rate during the preceding few Gigayears. There is observational evidence in favor of the latter (Forster Schreiber et al. 2009) Furthermore, if the clumps survive for a migration timescale, one expects most of the clumps at large disk radii to contain stellar populations younger than ~ 0.5 Gyr, while the clumps at smaller radii may also contain older populations. In contrast, if the clumps have lost their gas reservoir in less than ~ 100 Myr, they must have formed all their stars near the radius where they were formed and where they orbit for more than 1 Gyr, thus showing no obvious age gradient with radius. Finally, the massive radiation-driven outflows from clumps should be observable as systematic blueshifts at the clump locations. A preliminary search for such outflows yielded a null result (K. Shapiro, private communication).

10. GALAXY SIZE

As mentioned in §1, the observed SFG disks of $M_d \sim 10^{11} M_\odot$ at $z \sim 2$ are surprisingly extended, with radii ~ 10 kpc, comparable to the Milky Way today. These disk radii indicate $\lambda \sim 0.1$ in eq. (10) whereas the average value is expected to be smaller by a factor of 2 – 3 (Bullock et al. 2001a). We note that the proposed scenario of stream-driven unstable disks provides several possible explanations for the extended disk sizes, as well as for the compact spheroids.

The mass inflow in the disk into its center, by clump migration due to dynamical friction and encounters or by torques involving the transient shear and tidal features (§4), is associated with angular momentum transfer into the outer disk, which tends to stretch it further out. If the baryons in the bulge have lost all their angular momentum to the disk, by the time the bulge mass is comparable to the disk mass, the angular momentum per unit mass in the outer disk should be about twice the average, so the disk is expected to be twice as extended as it would have otherwise been. The timescale for reaching this state, eqs. (21) and (24), is on the order of one or two orbital times, namely a few hundred Megayears, and the configuration of comparable disk and bulge, $\delta \simeq 0.3$, is indeed the typical configuration expected in the clumpy steady state (§6).

Furthermore, in massive high- z disks that are fed by smooth streams, the generation of clumps and therefore the regions of intense star formation are expected to ex-

tend to the outer disk. First, the streams that determine the angular momentum of the disk tend to be coherent and to join the disk with an impact parameter comparable to the disk radius. They therefore generate high gas surface density Σ at large radii, as opposed to the exponential profiles of today's disks. The relative smoothness and low density of the high- z streams make them inefficient drivers of turbulence (§7), so they are not expected to push σ in the outer disk to high values. Finally, with a near flat rotation curve driven by the dark halo and the rather uniform disk outside the bulge, the angular velocity declines with radius roughly as $\Omega \propto r^{-1}$. These three factors allow $Q \propto \sigma\Omega/\Sigma$ to become low and admit instability at large radii. This is seen in simulated galaxies (Ceverino et al. 2009) and is consistent with the appearance of a broad, large-radius ring of giant clumps in some of the SFGs (Genzel et al. 2008).

The situation is very different in low-redshift disks. Unlike the halos at $z \sim 2$ that are fed by intense, coherent, narrow streams, a $10^{12} M_\odot$ halo at low redshift is fed from all directions by rather slow and erratic accretion (Kereš et al. 2005; Dekel & Birnboim 2006; Ocvirk et al. 2008; Dekel et al. 2009). The exponential profile tends to provide a sufficiently high Σ only at small radii, where the halo-driven rotation curve is closer to a solid-body rotation with a constant Ω , so the instability is not preferred at large radii.

Another possibly relevant mechanism is supernova feedback from early star formation in the central regions of galaxies. It is expected to be more effective at high redshift, when both the gas density and the SFR were higher. Supernova-driven winds may preferentially remove low angular momentum gas that has settled at earlier times in smaller radii, and thus leave behind a more extended system with higher angular momentum (Maller & Dekel 2002; Governato et al. 2007; Scannapieco et al. 2008).

Observations by Law et al. (2009) indicate that among the high-redshift galaxies with baryonic masses of a few $\times 10^{10} M_\odot$, slightly below the range of SFGs addressed in our paper, about a third seem to be supported by velocity dispersion rather than rotation, with $\sigma/V \sim 1/2 - 1$. These galaxies tend to be gas rich (up to 90%) and not overly extended, with typical radii $R \sim 1 - 2$ kpc. Such a galaxy could be formed if fed by cold flows of low impact parameters that carry little angular momentum. Alternatively, if these flows are overly clumpy, they could be effective in stirring up an excessively high dispersion in the gaseous galaxy. The absence of a substantial, unstable disk component in such a galaxy during its history may explain the relatively low past SFR and thus the observed high gas fraction.

11. GAS & STELLAR DISKS AT HIGH & LOW REDSHIFTS

The high-redshift disks are observed to be gas rich, at the level of 50% and perhaps more (Bouché et al. 2007; Daddi & et al., 2008). In contrast, today's massive disks are dominated by stars, with gas fractions of $\sim 20\%$ or less. Whereas both the gas and stellar components of the disk participate in the disk instability through their contributions to the local self-gravity, the gas dissipation introduces a long-term difference between the two components. While the decay of gas turbulence and gas cooling allow the velocity dispersion or sound speed to

decline even when the system is self-regulated and in a cosmological steady state, the stars tend to maintain the velocity dispersion that they have acquired during their history. The young stars may still have a σ that is not much larger than that of the gas, but the older stars are likely to have a higher σ . Therefore, the young stars actively participate in driving the perturbation growth and they may even follow the gas into the bound clumps, while the older stars tend to form transient perturbations and eventually join the stable component that just adds to the external potential well and thus helps stabilizing the disk.

The cosmological gas accretion rate plays an important role in determining the gas fraction in the disk. If stars form only in massive gas clumps, the disks are expected to remain gas rich as long as the gaseous input into the disk manages to replenish the disk mass on a timescale shorter than the time for the entire disk to turn into clumps, which is comparable to t_{evac} , namely

$$1 < \frac{(1-\gamma)\dot{M}_{\text{bar}}}{\dot{M}_{\text{evac}}} \simeq 0.24 \beta (1-\gamma) \alpha_2^{-1} Q^2 \delta^{-3} \tau. \quad (49)$$

The second equality is based on eqs. (21) and (26). For the unstable disk in steady state (§6.2), with $\gamma < 0.33$, this ratio is $\sim 2-3$ at $z \sim 2$, and it varies slowly with redshift. This implies that the disk should remain gas rich as long as the input is dominated by gas, which is more likely at high redshift. This indicates that the analysis performed in the current paper so far is a useful approximation for the high- z SFGs. At $z < 1.5$, the penetration of cold streams into the centers of halos more massive than $10^{12} M_{\odot}$ becomes limited (Dekel & Birnboim 2006; Ocvirk et al. 2008; ?), so the input rate of cold gas to the disks is lower than implied by eq. (25). At these late epochs, the fraction of stars in the accreting matter becomes higher. The disks gradually become dominated by the stars, in clumps and in transient features or spread out in the disk by shear and tidal stripping.

A more accurate analysis of disk instability, especially at low redshift, should therefore deal with multi-component disks. The axisymmetric instability of a two-component disk has been studied by Jog & Solomon (1984) and Rafikov (2001). Denoting the velocity dispersions of stars and gas σ_* and σ_g , respectively (with the latter standing for the speed of sound if thermal pressure dominates), and defining Q_* and Q_g following eq. (7) separately for each component, the effective Q relevant for the instability of the combined system is approximately

$$Q^{-1} = 2 Q_*^{-1} \frac{q}{1+q^2} + 2 Q_g^{-1} \frac{\sigma_{g*} q}{1+\sigma_{g*}^2 q^2}, \quad (50)$$

where $\sigma_{g*} \equiv \sigma_g/\sigma_*$ and q is the dimensionless wave number $q \equiv k\sigma_*/\kappa$. The first term has to be slightly modified to take into account the dissipationless nature of the stars⁶, but this correction makes only a small difference (Rafikov 2001). The system is unstable once $Q < 1$. The most unstable wavelength corresponds to the q that minimizes Q ; it lies between $q = 1$ for $\sigma_{g*} = 1$ and $q \simeq \sigma_{g*}^{-1}$ for $\sigma_{g*} \ll 1$. Note that with $\sigma_* > \sigma_g$, the stellar disk

by itself may tend to be less unstable than the gas disk by itself, $Q_* > Q_g$, but through its contribution to the self-gravity that drives the instability, the stellar disk can help the gas component de-stabilize the disk. The combined system can be unstable for axisymmetric perturbations even when each of the components has a Q value above unity.

If $\sigma_{g*} = 1$, the two components can be treated as one in the instability analysis. In order to illustrate the effect of different values of σ_{g*} , consider, for example, the case of equal mass densities for the gas and stars, $\Sigma_g = \Sigma_*$. When $\sigma_{g*} = 1$, the criterion for instability $Q < 1$ translates to $Q_g < 2$ (or $Q_* < 2$). If however the stars are “hotter”, $\sigma_{g*} = 0.5$ say, the criterion for instability (obtained at $q \simeq 1.6$) becomes $Q_g < 1.42$ (or $Q_* < 2.84$), so the error made in Q_c by ignoring the higher velocity dispersion of the stars (namely 2 versus 1.6) is about 30%. In this case, the instability driven by the cooler gas component is only slightly affected by the “hotter” stellar component. When the stellar disk is much “hotter” than the cold gas, $\sigma_{g*} \ll 1$, the instability criterion becomes $Q_g < 1$, so the stars become part of the stabilizing component of the system.

In the solar neighborhood, (according to Binney & Tremaine 2008, §6.2.3), the gas fraction is $\sim 25\%$, the stars are much “hotter” than the gas, $\sigma_{g*} \simeq 0.18$, and the separate Q values are $Q_g \simeq 1.5$ and $Q_* \simeq 2.7$. This gives a combined value of $Q \simeq 1.2$, indicating that the solar neighborhood is stable for axisymmetric perturbations because of the high velocity dispersion of the dominant stellar component. However, it is unstable for non-axisymmetric perturbations, only 20% variations in the surface density or the sound speed of the gas can generate axisymmetric instability.

We note that disk stabilization can be helped by the tendency of the gas temperature in the smooth, warm disk component not to drop significantly below 10^4K , corresponding to a speed of sound $\sim 15\text{km s}^{-1}$. This is because atomic cooling is ineffective at lower temperatures, and because supernova and stellar feedback tend to heat the gas to such temperatures (Wolfire et al. 2003). With $V \sim 200\text{km s}^{-1}$, such a minimum speed of sound would not allow Q to be kept below unity once $\delta < 0.13$. This implies that once the cold disk becomes less than 20% of the total baryonic mass, the disk tends to become stable against the formation of giant clumps.

Could the $z \sim 2$ thick disks of the SFGs evolve to the thick disks of today’s spiral galaxies? In the massive disk galaxies at low redshift, the thick disk is typically about a quarter of the total disk mass, and in smaller disks it could be as high as one half of the disk mass (Yoachim & Dalcanton 2006). If at $z \sim 2$ half the baryonic mass is in the disk ($\delta \sim 0.3$) that becomes the thick stellar disk of today, and if, say, the total baryonic mass has doubled since then and all of it has settled in a new thin disk, then today’s thick disk fraction is expected to be about a third, marginally consistent with the observed fractions. On the other hand, the velocity dispersion in the high- z stellar disks might be too high to be consistent with today’s thick disks. Many of them may end up as S0 galaxies, or as elliptical galaxies if they go through significant mergers. The simulations described in §12 (Ceverino et al. 2009) indeed demonstrate that the evo-

⁶ for a dissipationless component, the q dependence in the first term should be replaced by $q^{-1}[1 - \exp(-q^2)I_0(q^2)]$, where I_0 is the Bessel function of order 0.

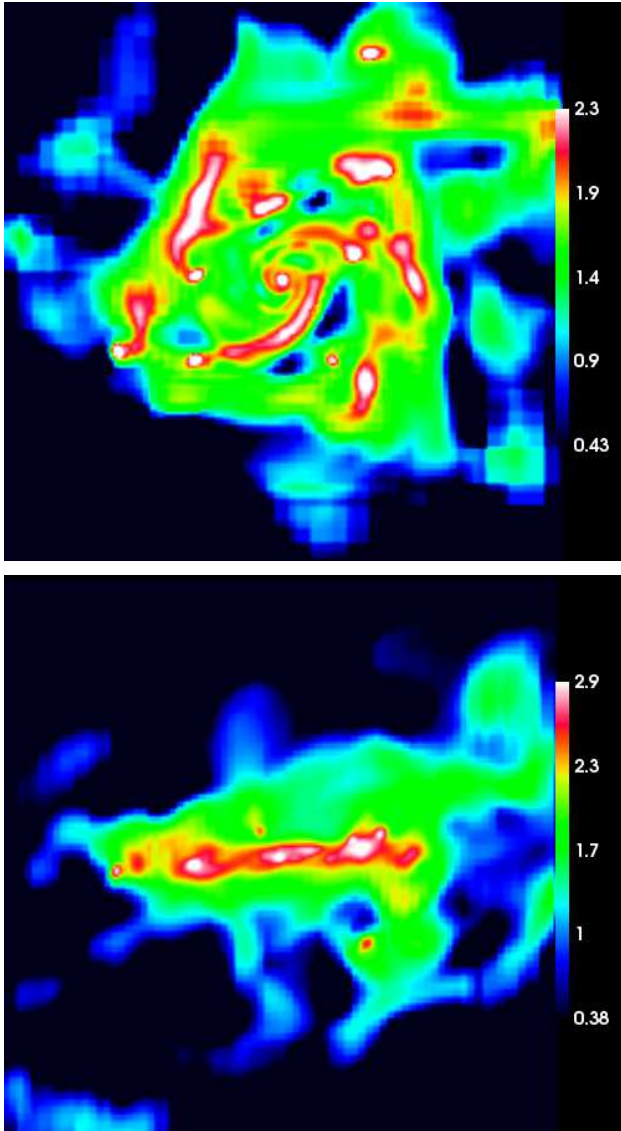


FIG. 2.— Gas surface density of a galaxy at $z \sim 2.3$ from a high-resolution cosmological simulation (Ceverino et al. 2009). The box side is 15 kpc. The color code is log surface density in units of $M_{\odot} \text{pc}^{-2}$. Only gas with density $n > 0.1 \text{cm}^{-3}$ is shown. The face-on view (top) shows an extended disk broken into several giant clumps and sheared perturbations, similar to many observed SFGs. The edge-on view demonstrates that this is a well defined disk, resembling the observed “chain” systems. The disk is fed by streams, not emphasized in this picture because they are largely below the threshold density for the plot. With $\delta \simeq 0.26$, this system is in a steady state at the late stages of the clump-instability phase. This galaxy, in a halo of $4 \times 10^{11} M_{\odot}$, is smaller than the typical SFG, but it resembles the typical appearance of SFGs and it demonstrates the general behavior predicted by our theoretical analysis.

lution into an S0-like configuration is likely. However, it is clear that not all the massive high-redshift SFGs end up as S0’s today, because the mean comoving number density of SFGs ($\gtrsim 10^{-4} \text{Mpc}$) is higher than that of today’s S0’s ($< 10^{-4} \text{Mpc}$).

12. COSMOLOGICAL SIMULATIONS

Figure 2 provides a sneak preview of the results from zoom-in cosmological simulations that are analyzed in

more detail in a companion paper (Ceverino et al. 2009). Shown are the first maps of gas density in a properly resolved galaxy at $z \simeq 2.3$, which clearly show a disk broken into giant clumps and sheared features. They are brought here for the sake of demonstrating the validity of the simple analysis presented above.

These zoom-in cosmological simulations are performed about individual galaxies using a Hydrodynamic Adaptive Refinement Tree code (Kravtsov et al. 1997; Kravtsov 2003) with a spatial resolution better than 70 pc (in physical units). The code incorporates the relevant physical processes, including atomic and molecular gas cooling and photoionization heating, star formation, metal enrichment, and feedback from stars and supernovae, as described in Ceverino & Klypin (2009). The unique feature of this code for the purpose of simulating disk instability is that it allows the gas to cool down to $\sim 100 \text{K}$. This is a key to resolving the turbulence Jeans mass and permitting the disk fragmentation into giant clumps, not seen before in cosmological simulations.

The galaxy shown in Fig. 2 is one of a few simulated galaxies, most of which showing similar features, although they are on the small side of the massive SFGs observed (as they were originally selected for another purpose, to match a virial mass of $10^{12} M_{\odot}$ at $z = 1$). In the specific case shown, at $z = 2.3$, the halo virial parameters are $M_v \simeq 4 \times 10^{11} M_{\odot}$ and $R_v \simeq 70 \text{kpc}$. The disk extends to $R_d \simeq 6 \text{kpc}$ with a rather flat rotation curve of $V \simeq 180 \text{km s}^{-1}$. The disk mass is $M_d \simeq 1.1 \times 10^{10} M_{\odot}$, in comparable fractions of gas and stars. The stellar spheroid is $M_{\text{sph}} \simeq 1.0 \times 10^{10} M_{\odot}$, and the total mass within R_d is $M_{\text{tot}} \simeq 4.2 \times 10^{10} M_{\odot}$, so the disk-to-total ratio is $\delta \simeq 0.26$. This value is near the predicted steady-state value for $\gamma \lesssim 0.33$.

The map clearly reveals a disk configuration dominated by a few giant clumps, containing a fraction $\alpha \simeq 0.12$ of the disk mass. By inspecting the time evolution of this galaxy, we deduce that most of the clumps seen in the map were formed in situ in the disk, and only two of them came from outside. These two are embedded in dark-matter halos while all the other clumps are “naked” baryonic clumps. The edge-on view shows that the clump deviation from the mid-plane is comparable to and smaller than the intrinsic disk thickness. This is both evidence for in situ clump formation and a typical characteristic of observed “chain” galaxies (Elmegreen & Elmegreen 2006). With the bulge comparable to the disk, with the stellar component already quite developed, and with a non-negligible clumpiness of $\gamma \simeq 0.2$ in the incoming streams, this galaxy seems to be at a late stage of its giant-clump phase. The value of Q for the combined gas and stellar disk is below unity in parts of a ring of radius $\sim 5 \text{kpc}$, but it is above unity for the disk as a whole. This may indicate that this system is at a stage where it is gradually becoming stable against axisymmetric perturbations by its old stellar component. Indeed, by the end of this simulation at $z = 1.3$, the galaxy becomes dominated by its stellar spheroid with only a minor, rather stable gas disk. Note, however, that the comparison of the linear instability analysis with the simulated clumpy disk should be interpreted with care, taking into account the fact that the linear analysis is valid at the onset of instability while the quantities quoted above are measured

from the highly perturbed disk.

Convergence tests that are described in detail in Ceverino et al. (2009) demonstrate that the in situ clumps are a result of a real physical fragmentation process and not a numerical artifact. In order to prevent artificial fragmentation due to an unresolved Jeans scale, we implemented in the code a standard procedure that imposes a pressure floor (not by means of a temperature floor), which prevents the Jeans length from falling below $\lambda_J = N_J \Delta$, where Δ is the cell size of the numerical grid. The standard value is $N_J = 4$ for simulations that last a dynamical time (Truelove et al. 1997). To verify the minimum value of N_J that prevents artificial fragmentation in a disk that evolves for several dynamical times, we repeated our simulation for 400 Myr with the same resolution but using N_J values that range from 1 to 10. We found that the mass in clumps and the number of clumps converge to constant values for $N_J = 7-10$, while there is an overproduction of clumps that worsens with decreasing N_J in the range $N_J = 1-7$. This indicates that the clumps represent a real physical phenomenon once $N_J \geq 7$, so we adopt $N_J = 7$ for our default analysis.

? have reported independently and immediately after us a similarly clumpy disk in their own simulation of a galaxy in a cosmological background, using an AMR code very similar to ours and with a comparable resolution. Applying $N_J = 4$ for the pressure floor, they indeed find more and typically smaller clumps, as expected from our numerical tests. We conclude that while their simulation may be partly subject to numerical fragmentation, they basically detect the same real physical phenomenon that we see in our simulations.

13. SUMMARY AND DISCUSSION

We studied the Toomre instability of high-redshift, gas-dominated, massive, thick, galactic disks as they are intensely fed by cosmological cold streams. Defining the disk fraction $\delta \equiv M_d/M_{\text{tot}}(R_d)$, an unstable disk *self-regulates* itself to $Q \simeq Q_c \sim 1$ with a velocity dispersion $\sigma_r/V \simeq Q_c \delta / \sqrt{3}$. The disk develops transient elongated sheared features, and fragments into a few in situ bound massive clumps, each a few percents of the disk mass and together involving a fraction $\alpha \sim 0.2$ of the disk mass. The turbulence is largely maintained by the internal gravitational interactions within the perturbed disk. In particular, the encounters between the disk clumps stir up velocity dispersion on a timescale $t_{\text{enc}} \simeq 2.1 Q^2 \alpha^{-1} t_d$, where $t_d \equiv \Omega^{-1} \simeq 50$ Myr, which is sufficient by itself for matching the natural timescale for turbulence decay, $t_{\text{dis}} \simeq 1.4 Q^{-1} t_d$, once $Q \simeq 0.67$ and $\alpha \simeq 0.2$.

The same gravitational encounters and dynamical friction make the giant clumps *migrate* to the center on a timescale $t_{\text{mig}} \simeq 2.1 Q^2 \delta^{-2} t_d$ and grow a bulge. The associated evacuation timescale for the entire disk mass is $t_{\text{vac}} \simeq 10.5 \alpha^{-1} Q^2 \delta^{-2} t_d$, which is comparable to the timescale for mass inflow due to torques of the transient features.

The cosmological streams feed baryons to the galaxy on a timescale $t_{\text{acc}} \simeq 44 \tau^{-1} t_d$, with $\tau \simeq 1$ at $z = 2$ (and varying from 0.4 to 2.5 between $z \simeq 1$ and 9). The smooth component of the incoming streams, including small clumps, replenishes the evacuating disk, while the external massive clumps associated with the streams

merge to the bulge. If the galaxy is fed by streams that contain less massive clumps than average, $\gamma < 0.33$, the system settles into a near *steady state* with $\delta \simeq 0.3$, where the input by streams and the transport from disk to bulge maintain a constant bulge-to-disk ratio near unity.

In galaxies where the incoming streams are more clumpy than critical, $\gamma > 0.33$, the external massive clumps merge into a dominant spheroid, $\delta < 0.3$, and the dense clumps stir-up the turbulence in the disk to levels that *stabilize* the disk. The dependence of the instability on the degree of clumpiness in the streams introduces a *bimodality* in the galaxy properties starting already at $z \geq 3$. Streams smoother than average lead to extended, unstable disks with giant in situ clumps that form stars at a high rate, while more clumpy streams help building compact, massive bulges and stir up the disks to stabilization followed by suppressed SFR, as follows.

In about half the halos of $\sim 10^{12} M_\odot$ at $z > 1$, where the streams are relatively smooth, the rapid accretion at high z leads to a dense, gas-dominated disk with $\delta \lesssim \beta \simeq 0.6$. Such a disk is wildly unstable; it grows sheared perturbations and fragments into a few giant clumps, each comprising a few percent of the disk mass. The clump interactions self-regulate the disk in a marginally unstable state, with $Q \simeq Q_c$. The clumps migrate inward in a couple of rotation times and form a spheroid. The combined effects of penetrating streams, disk evacuation and spheroid growth make δ approach a near steady state within one Hubble time. They maintain the giant-clump phase with $\delta \sim 0.3$ and $\sigma_r/V \simeq 0.15 - 0.3$ for several Gigayears, till well after $z \sim 2$. During this phase, as the accretion rate gradually slows down, the bulge-to-disk ratio grows slowly, the velocity dispersion σ_r/V declines accordingly to keep $Q \simeq Q_c$, the clumps get slightly smaller in proportion to δ^2 , and the clump migration and disk evacuation slow down by a similar small factor.

In the other half of the massive galaxies, where the clumpy component of the streams is higher than average, the dense clumps stir up turbulence in the disk at a level that can stabilize the disk against the formation of giant clumps once the bulge is more massive than the disk. Even if the system starts as an unstable disk forming stars at a very high redshift, once fed by clumpy streams it settles within a Hubble time to a phase of growth where the disk is stabilized. In this case, most of the star formation and the most rapid growth of the spheroid occurred during the first Gigayear or two. Once the disk is stable, it does not form new clumps, and when the remaining disk clumps have consumed most of their gas or disappeared, the SFR is substantially suppressed.⁷

The proposed picture has interesting implications on the sizes of galaxies at high redshift. After the system have grown a bulge comparable to the disk, the disk is expected to be twice as extended as implied by the standard spin-parameter argument, because it acquired the angular momentum lost by the material that migrated to the bulge. Another reason for the extended appearance of the disk is that the coherent streams tend to join the disks in their outer parts. This makes the generation of

⁷ This is yet another context where clumpy streams help the quenching in massive halos where the potential well is deep (Dekel & Birnboim 2008; Khochfar & Silk 2009).

clumps and the resulting star formation most efficient in an outer ring. In turn, the typical high-redshift spheroids are expected to be compact because the timescales for in situ clump migration, as well as the timescale for incoming mergers, are comparable to the star formation time in the clumps, making the coalescence into the bulge highly dissipative.

The disk giant clumps are the sites of intense star formation, in an overall rate that follows the gas accretion rate of $\sim 100 M_{\odot} \text{yr}^{-1}$ at $z \sim 2$. The apparent star formation efficiency in the clumps is $\eta \sim 0.1$ compared to star formation on a dynamical time. For a local efficiency at a standard level of $\lesssim 1\%$, as observed in star-forming molecular clouds, the star formation has to be confined to a cuspy core or subclumps that are denser than their host giant clumps by one to two orders of magnitudes.

The giant clumps are not expected to be disrupted by supernova feedback, but a significant fraction of their gas may be expelled back to the disk by radiative stellar feedback (Murray et al. 2009). This would not change the predicted steady state in a qualitative way, but it would slow down the bulge growth, leaving mergers as the dominant mechanism for spheroid formation. The distribution of stellar ages within the individual disk clumps can provide an observational constraint on the actual level of clump disruption prior to their coalescence with the central bulge. If the clumps indeed underwent an effective gas removal, the spread of ages within each clump is not expected to exceed ~ 100 Myr, and the outflows from the clumps should be detectable observationally.

If clump disruption is not too effective during their migration, the efficient formation of bulges by clump migration in the high-redshift disks helps reconciling the models of galaxy formation with the observed abundance of stellar spheroids. The cosmological major-merger rate seems insufficient for the purpose (e.g., Jogee 2008; Dekel et al. 2009; Bundy et al. 2009). Indeed, not having enough mergers in the simulations, most semi-analytic models of galaxy formation had to assume a high rate of bulge growth from disk instabilities in order to match the observed abundance of spheroids (Cattaneo et al. 2008; Parry et al. 2009). Our analysis spells out the origin of this instability.

As proposed by Elmegreen et al. (2008b), the massive black holes observed in spheroids already at high redshift can naturally originate from seed black holes that have formed by massive-star coalescence in the dense stellar clusters at the centers of the giant clumps. These black holes were shown to migrate with the clumps into the central spheroid, and to reproduce the observed black hole to spheroid mass ratio of $\sim 10^{-3}$. The AGN feedback associated with the central black hole can add yet another quenching mechanism (Cattaneo et al. 2009), which also becomes more effective as the bulge grows.

If the properties of the streams feeding a given galaxy vary in time, and in particular if the degree of clumpiness in them evolves, the galaxy may go through transitions from an unstable disk-dominated configuration to a stable bulge-dominated state and vice versa. However, after $z \sim 2$, the recovery from a bulge-dominated system back to an unstable disk takes several Gigayear and may never materialize.

A systematic change in the stream properties is expected after $z \sim 1$, where the cosmological accretion rate

becomes slower and the smooth cold streams no longer penetrate very effectively through the shock-heated media in massive halos of $\sim 10^{12} M_{\odot}$ or higher (Kereš et al. 2005; Dekel & Birnboim 2006; Cattaneo et al. 2006; Ocvirk et al. 2008). Once the accretion cannot replenish the disks on a time scale comparable to the timescale for the disks to turn into clumps and stars, the galaxies become *star dominated* and eventually stable against axisymmetric modes. Supernova and stellar feedback can then add to the stabilization of the gas disk. The common late disks form predominantly in halos below the threshold mass of $\sim 10^{12} M_{\odot}$, and not necessarily by narrow streams (Birnboim & Dekel 2003; Binney 2004; Kereš et al. 2005; Dekel & Birnboim 2006; Birnboim et al. 2007). They evolve secularly through non-axisymmetric modes of instability associated with quiescent star formation. The turbulent high-redshift disks may end up in today's thick disks and S0 galaxies, or in ellipticals through mergers. The spheroids continue to grow according to the standard scenario; bulges develop by slow secular evolution in the disks (Bureau & Athanassoula 2005; Athanassoula 2008), and all spheroids, including today's giant ellipticals, grow by minor and major mergers.

We conclude that the typical high-redshift massive galaxies are in a phase of evolution that does not have a common parallel in low-redshift galaxies. On one hand, the intense and deeply penetrating coherent, cold gas streams keep the disk gas rich and thus drive a wild instability with giant clumps forming stars at a high rate, and maintain this phase in steady state for cosmological times. In parallel, a high degree of clumpiness in some of the high-flux streams could stabilize the disks against the formation of giant clumps and form massive spheroids with low SFR already at high redshift. We note, however, that there are rare cases at low redshift of relatively gas-rich galaxies that somewhat resemble the perturbed clumpy appearance of the high-redshift SFGs (e.g., NGC 4303, Boissier et al. 2003). They may be scaled down versions of the SFGs, possibly unstable to axisymmetric modes but with much lower gas densities and SFR, and probably fed by overly intense accretion compared to the average at low redshift.

The quenching of disk star formation by a dominant stellar bulge, which can be termed “morphological quenching”, is addressed and demonstrated using simulations in Martig et al. (2009). It can explain the existence of red-and-dead early-type galaxies in the field, that is in halos below the critical mass for virial shock heating, above which the quenching can be explained in other ways involving termination of gas supply (Dekel & Birnboim 2006). Morphological quenching predicts the presence of non-negligible stable gas disks in some of the field early-type galaxies.

Preliminary tests indicate that the theoretical framework proposed here is in general agreement with the evolution of galaxies in hydrodynamical cosmological simulations of appropriate resolution (Ceverino et al. 2009), as well as with the observations of high-redshift galaxies. However, the comparison of the linear instability analysis with the evolved, nonlinearly perturbed systems, as simulated or as observed, should be performed with care. Our current analysis is meant to provide a simple, basic, theoretical framework, but the exact numeri-

cal values quoted for the parameters, averaged over the whole disk, should not be interpreted too literally. The simulations allow us to predict the observable appearance of the cold streams that drive galaxy formation at high redshift, either in emission as Lyman-alpha Blobs (Dijkstra & Loeb 2009; Goerdt et al. 2009), or in absorption as Lyman-limit systems or Damped Lyman-alpha systems (Dekel et al. 2009).

We acknowledge stimulating discussions with Fred-

eric Bournaud, Andi Burkert, Bruce Elmegreen, Reinhard Genzel, Peter Goldreich, Tobias Goerdt, Mark Krumholz, Doug Lin, Norm Murray and Amiel Sternberg. This research has been partly supported by an ISF grant, by GIF I-895-207.7/2005, by a DIP grant, by a France-Israel Teamwork in Sciences, by the Einstein Center at HU, by NASA ATP NAG5-8218 at UCSC, and by an ERC Starting Grant (RS).

APPENDIX

STEADY STATE: APPROXIMATE SOLUTIONS

In the limit $4b^3/(27c^2) \ll 1$, the expression in eq. (38) becomes $u \simeq c^{1/3}$. In our fiducial case at $z \simeq 2$, this limit corresponds to $(1 - \gamma)^2 \gg 4/27$, namely smooth streams, leading to steady state with the disk more massive than the bulge. For $0 \leq \gamma \leq 0.33$ (where $0.33 \geq \delta_{\text{ss}} \geq 0.26$), this approximation underestimates δ_{ss} by a few percent.

In the other limit, $c^2/b^3 \ll 1$, there is an approximate solution of the sort $\delta_{\text{ss}} = (c/b)(1 - \epsilon)$ with $\epsilon \ll 1$; to first order in ϵ it is $\epsilon \simeq c^2 b^{-3}/(1 + 3c^2 b^{-3})$. In our fiducial case at $z \simeq 2$, this limit corresponds to $(1 - \gamma)^2 \ll 1$, namely clumpy streams, leading to steady state with a dominant bulge. This approximation overestimates δ_{ss} by a few percent for $\gamma \geq 0.3$ ($\delta_{\text{ss}} \leq 0.27$).

The general behavior of the solution of eq. (32) can be evaluated analytically in the fiducial case when noticing that the second term involving t_{acc} becomes negligible near $\delta \simeq \beta(1 - \gamma)$, that is $\simeq 0.33$ for the fiducial case, not far from the steady-state value. With $t_{\text{d}} \propto t$, the simplified equation $\dot{\delta} \simeq -t_{\text{evac}}^{-1} \delta$ becomes $\dot{\delta}/\delta^3 \simeq -6.33 \alpha_{.2} \lambda_{.1}^{-1} t^{-1}$, and its solution is

$$\delta^{-2} - \delta_{\text{in}}^{-2} \simeq 12.7 \alpha_{.2} \lambda_{.1}^{-1} \ln(t/t_{\text{in}}). \quad (\text{A1})$$

According to this, with $\delta_{\text{in}} \simeq 0.5$, the system is expected to evolve to near δ_{ss} by $t \simeq 2t_{\text{in}}$, as seen in the exact solution, Fig. 1.

If we assume instead that t_{d} is the same at all times, the equation is replaced by $\dot{\delta}/\delta^3 \simeq -2.0 \alpha_{.2} t_{48}^{-1}$ and the solution becomes

$$\delta^{-2} - \delta_{\text{in}}^{-2} \simeq 4.0 \alpha_{.2} t_{48}^{-1} (t - t_{\text{in}}). \quad (\text{A2})$$

Again, the system is expected to evolve rapidly to near steady state, crudely reproducing the behavior in Fig. 1.

The term neglected in eq. (32) tends to add a negative contribution to $\dot{\delta}$ for $\delta > \beta(1 - \gamma)$, and a positive contribution for smaller values of δ . This speeds up the evolution when the system is far from the steady state value, and it may either speed it up or slow it down near steady state.

COMMENTS ON THE ORIGIN OF PRESSURE SUPPORT

Since the gas cools rapidly to 10^4K , the thermal pressure cannot support a clump of $\sigma_r \simeq 30 \text{ km s}^{-1}$ against gravitational collapse and star formation on a free-fall time. The required pressure support must be due to velocity dispersion. Can the gravitational interactions in the perturbed disk drive the turbulence inside the clumps? We address this issue using simulations elsewhere, and bring only two preliminary considerations here.

The dissipation rate of turbulence inside a rather uniform gas clump is

$$\dot{E}_{\text{dis}} \simeq \frac{1.2 M_c \sigma_c^3}{0.5 R_c} \simeq 2.4 M_c \sigma_c^2 t_{\text{d}}^{-1}, \quad (\text{B1})$$

assuming a radius $0.5R_c$ for the clump, and using in the second equality $R_c/\sigma_c \simeq t_{\text{d}}$ with t_{d} the disk dynamical time. The associated timescale is $t_{\text{dis}} \simeq 0.6R_c/\sigma_c$, i.e., comparable to the dynamical time of the clump, $t_c \sim 0.5t_{\text{d}}$. In comparison, the rate of gravitational work done on the clump as it migrates a radial distance R_{d} is

$$\dot{E}_{\text{mig}} \simeq \frac{GM_{\text{tot}}M_c}{R_{\text{d}} t_{\text{mig}}} \simeq 0.5 M_c V^2 Q^{-2} \delta^2 t_{\text{d}}^{-1}. \quad (\text{B2})$$

The ratio of the two is $\dot{E}_{\text{dis}}/\dot{E}_{\text{mig}} \simeq 1.7 Q^4$, which is of order unity for $Q \sim 1$ and about a third for our fiducial $Q = 0.67$. This implies that the gravitational power associated with the migration is in principle enough for balancing the turbulence decay inside the clumps. The actual mechanism for pumping up the internal energy in the clumps could in principle be clump encounters, shear and tidal interactions with the transient perturbations, yet to be studied in detail.

The decay of turbulence within the clumps may actually be slower than implied by eq. (B1) and thus easier to balance. For example, the dissipation rate naturally slows down in proportion to the gas fraction as the gas turns into stars. The fragmentation to dense subclumps, advocated in §8, may have a similar effect by itself. If the giant clump

fragments to N_{sub} subclumps of equal mass in which the gas density is n_{sub} , the turbulence decay rate would change in proportion to the total cross section for subclump collisions,

$$\dot{E}_{\text{dis}} \propto N_{\text{sub}} \frac{R_{\text{sub}}^2}{R_c^2} \propto \left(\frac{n_c}{n_{\text{sub}}} \right)^{2/3} N_{\text{sub}}^{1/3}. \quad (\text{B3})$$

If $n_{\text{sub}}/n_c \sim 36$, to allow $\eta \sim 0.01$ in the subclumps (§8), we obtain that the turbulence decay would slow down as long as $N_c < 10^3$. This implies for $10^9 M_\odot$ clumps that the dissipation timescale would be longer than the clump dynamical time as long as the actual gas clouds forming stars are bigger than $10^6 M_\odot$.

REFERENCES

- Adelberger, K. L., Steidel, C. C., Shapley, A. E., Hunt, M. P., Erb, D. K., Reddy, N. A., & Pettini, M. 2004, *ApJ*, 607, 226
- Agertz, O., Lake, G., Teyssier, R., Moore, B., Mayer, L., & Romeo, A. B. 2008, *MNRAS*, 1373
- Athanassoula, E. 2008, in *ASP Conf. S.*, Vol. 396, *Formation and Evolution of Galaxy Disks*, ed. J. G. Funes & E. M. Corsini (San Francisco, CA: ASP)
- Binney, J. 2004, *MNRAS*, 347, 1093
- Binney, J., & Tremaine, S. 2008, *Galactic Dynamics* (Princeton, NJ, Princeton Univ. Press)
- Birnboim, Y., & Dekel, A. 2003, *MNRAS*, 345, 349
- Birnboim, Y., Dekel, A., & Neistein, E. 2007, *MNRAS*, 380, 339
- Blumenthal, G. R., Faber, S. M., Primack, J. R., & Rees, M. J. 1984, *Nature*, 311, 517
- Boissier, S., Prantzos, N., Boselli, A., & Gavazzi, G. 2003, *MNRAS*, 346, 1215
- Bouché, N. et al. 2007, *ApJ*, 671, 303
- Bournaud, F. et al. 2008, *A&A*, 486, 741
- Bournaud, F., & Elmegreen, B. G. 2009, *ApJ*, 694, L158
- Bournaud, F., Elmegreen, B. G., & Elmegreen, D. M. 2007, *ApJ*, 670, 237
- Bullock, J. S., Dekel, A., Kolatt, T. S., Kravtsov, A. V., Klypin, A. A., Porciani, C., & Primack, J. R. 2001a, *ApJ*, 555, 240
- Bullock, J. S., Kolatt, T. S., Sigad, Y., Somerville, R. S., Kravtsov, A. V., Klypin, A. A., Primack, J. R., & Dekel, A. 2001b, *MNRAS*, 321, 559
- Bundy, K., Fukugita, M., Ellis, R. S., Targett, T. A., Belli, S., & Kodama, T. 2009, *ApJ*, 697, 1369
- Bureau, M., & Athanassoula, E. 2005, *ApJ*, 626, 159
- Cattaneo, A., Dekel, A., Devriendt, J., Guiderdoni, B., & Blaizot, J. 2006, *MNRAS*, 370, 1651
- Cattaneo, A., Dekel, A., Faber, S. M., & Guiderdoni, B. 2008, *MNRAS*, 389, 567
- Cattaneo, A., Faber, S. M., Binney, J., Dekel, A., Kormendy, J., & Mushotzky, R. 2009, *Nature*, 460, 213
- Ceverino, D., Dekel, A., & Bournaud, F. 2009, *ArXiv:0907.3271*
- Ceverino, D., & Klypin, A. 2009, *ApJ*, 695, 292
- Chapman, S. C., Smail, I., Blain, A. W., & Ivison, R. J. 2004, *ApJ*, 614, 671
- Covington, M., Dekel, A., Cox, T. J., Jonsson, P., & Primack, J. R. 2008, *MNRAS*, 384, 94
- Daddi, E., Cimatti, A., Renzini, A., Fontana, A., Mignoli, M., Pozzetti, L., Tozzi, P., & Zamorani, G. 2004, *ApJ*, 617, 746
- Daddi, E., & et al.. 2008, *ApJ*, 673, L21
- Dekel, A., & Birnboim, Y. 2006, *MNRAS*, 368, 2
- . 2008, *MNRAS*, 383, 119
- Dekel, A. et al. 2009, *Nature*, 457, 451, *ArXiv:0808.0553*
- Dekel, A., & Cox, T. J. 2006, *MNRAS*, 370, 1445
- Dekel, A., & Silk, J. 1986, *ApJ*, 303, 39
- Dijkstra, M., & Loeb, A. 2009, *ArXiv:0902.2999*
- Elmegreen, B. G., Bournaud, F., & Elmegreen, D. M. 2008a, *ApJ*, 688, 67
- . 2008b, *ApJ*, 684, 829
- Elmegreen, B. G., & Elmegreen, D. M. 2005, *ApJ*, 627, 632
- . 2006, *ApJ*, 650, 644
- Elmegreen, B. G., Elmegreen, D. M., Ximena Fernandez, M., & Lemonias, J. J. 2008c, *ApJ*, 691, 23
- . 2009, *ApJ*, 692, 12
- Elmegreen, D. M., Elmegreen, B. G., & Hirst, A. C. 2004, *ApJ*, 604, L21
- Elmegreen, D. M., Elmegreen, B. G., Ravindranath, S., & Coe, D. A. 2007, *ApJ*, 658, 763
- Fall, S. M. 1979, *Nature*, 281, 200
- Fall, S. M., & Efstathiou, G. 1980, *MNRAS*, 193, 189
- Forster Schreiber, N. M. et al. 2009, *ArXiv:0903.1872*
- Forster Schreiber, N. M. et al. 2006, *ApJ*, 645, 1062
- Gammie, C. F. 2001, *ApJ*, 553, 174
- Genel, S. et al. 2008, *ApJ*, 688, 789
- Genzel, R. et al. 2008, *ApJ*, 687, 59
- . 2006, *Nature*, 442, 786
- Goerdt, T., Dekel, A., Sternverg, A., Ceverino, D., Teyssier, R., & Primack, R. 2009, *ArXiv:0909.0000*
- Goldreich, P., & Lynden-Bell, D. 1965a, *MNRAS*, 130, 97
- . 1965b, *MNRAS*, 130, 125
- Goldreich, P., & Tremaine, S. 1980, *ApJ*, 241, 425
- Governato, F. et al. 2009, *MNRAS*, 397, 957
- Governato, F., Willman, B., Mayer, L., Brooks, A., Stinson, G., Valenzuela, O., Wadsley, J., & Quinn, T. 2007, *MNRAS*, 374, 1479
- Hopkins, P. F., Bundy, K., Hernquist, L., & Ellis, R. S. 2007, *ApJ*, 659, 976
- Immeli, A., Samland, M., Gerhard, O., & Westera, P. 2004a, *A&A*, 413, 547
- Immeli, A., Samland, M., Westera, P., & Gerhard, O. 2004b, *ApJ*, 611, 20
- Jog, C. J., & Solomon, P. M. 1984, *ApJ*, 276, 127
- Jogee, S. 2008, *ArXiv:0810.5617*
- Kennicutt, R. C. 1989, *ApJ*, 344, 685
- Kereš, D., Katz, N., Weinberg, D. H., & Davé, R. 2005, *MNRAS*, 363, 2
- Khochfar, S., & Silk, J. 2009, *ApJ*, 700, L21
- Kravtsov, A. V. 2003, *ApJ*, 590, L1
- Kravtsov, A. V., Klypin, A. A., & Khokhlov, A. M. 1997, *ApJS*, 111, 73
- Kriek, M. et al. 2006, *ApJ*, 649, L71
- Krumholz, M. R., McKee, C. F., & Tumlinson, J. 2009, *ApJ*, 699, 850
- Law, D. R., Wright, S. A., Ellis, R. S., Erb, D. K., Nesvadba, N., Steidel, C. C., & Swinbank, M. 2009, *Astronomy*, 2010, 172
- Lehnert, M. D., Nesvadba, N. P. H., Tiran, L. L., Matteu, P. D., van Driel, W., Douglas, L. S., Chemin, L., & Bournaud, F. 2009, *ApJ*, 699, 1660
- Maller, A. H., & Dekel, A. 2002, *MNRAS*, 335, 487
- Martig, M., Bournaud, F., Teyssier, R., & Dekel, A. 2009, *ArXiv:0905.4669*
- Mo, H. J., Mao, S., & White, S. D. M. 1998, *MNRAS*, 295, 319
- Murray, N., Quataert, E., & Thompson, T. A. 2009, *ArXiv:0906.5358*
- Neistein, E., & Dekel, A. 2008, *MNRAS*, 383, 615
- Neistein, E., van den Bosch, F. C., & Dekel, A. 2006, *MNRAS*, 372, 933
- Noguchi, M. 1999, *ApJ*, 514, 77
- Ocvirk, P., Pichon, C., & Teyssier, R. 2008, *MNRAS*, 390, 1326
- Parry, O. H., Eke, V. R., & Frenk, C. S. 2009, *MNRAS*, 396, 1972
- Rafikov, R. R. 2001, *MNRAS*, 323, 445
- Robertson, B., Bullock, J. S., Cox, T. J., Di Matteo, T., Hernquist, L., Springel, V., & Yoshida, N. 2006, *ApJ*, 645, 986
- Robertson, B. E., & Bullock, J. S. 2008, *ApJ*, 685, L27
- Sari, R., & Goldreich, P. 2004, *ApJ*, 606, L77
- Scannapieco, C., Tissera, P. B., White, S. D. M., & Springel, V. 2008, *MNRAS*, 389, 1137
- Shakura, N. I., & Sunyaev, R. A. 1973, *A&A*, 24, 337
- Shapiro, K. L. et al. 2008, *ApJ*, 682, 231
- Springel, V., & Hernquist, L. 2005, *ApJ*, 622, L9
- Stark, D. P., Swinbank, A. M., Ellis, R. S., Dye, S., Smail, I. R., & Richard, J. 2008, *Nature*, 455, 775

- Tacconi, L. J. et al. 2008, *ApJ*, 680, 246
Tasker, E. J., & Bryan, G. L. 2008, *ApJ*, 673, 810
Tasker, E. J., & Tan, J. C. 2009, *ApJ*, 700, 358
Toomre, A. 1964, *ApJ*, 139, 1217
Toomre, A., & Toomre, J. 1972, *ApJ*, 178, 623
Truelove, J. K., Klein, R. I., McKee, C. F., Holliman, II, J. H.,
Howell, L. H., & Greenough, J. A. 1997, *ApJ*, 489, L179
van den Bergh, S., Abraham, R. G., Ellis, R. S., Tanvir, N. R.,
Santiago, B. X., & Glazebrook, K. G. 1996, *AJ*, 112, 359
van Dokkum, P. G. et al. 2008, *ApJ*, 677, L5
van Starckenburg, L., van der Werf, P. P., Franx, M., Labbé, I.,
Rudnick, G., & Wuyts, S. 2008, *A&A*, 488, 99
Wada, K., Meurer, G., & Norman, C. A. 2002, *ApJ*, 577, 197
Wall, J. V., Pope, A., & Scott, D. 2008, *MNRAS*, 383, 435
Ward, W. R. 1997, *Icarus*, 126, 261
White, S. D. M., & Rees, M. J. 1978, *MNRAS*, 183, 341
Wolfire, M. G., McKee, C. F., Hollenbach, D., & Tielens,
A. G. G. M. 2003, *ApJ*, 587, 278
Yoachim, P., & Dalcanton, J. J. 2006, *AJ*, 131, 226